PC1

GLUT2 expression at the rat proximal tubule brush border membrane correlates with plasma glucose concentration

J. Marks[1], A.K. Goestemeyer[1], E.S. Debnam[1], S.K. Srai[2] and R.J. Unwin[3,1]

[1]Physiology, Royal Free And University College Medical School, London, UK, [2]Biochemistry, Royal Free And University College Medical School, London, UK and [3]Nephrology, Royal Free And University College Medical School, London, UK

There is increasing evidence that in the kidney and small intestine, expression levels of the facilitative glucose transporters are influenced by changes in plasma glucose concentrations. Indeed, our previous studies have reported increased GLUT2 expression at the proximal tubule brush border membrane (BBM) of animals with streptozotocin (STZ)-induced Type 1 diabetes. Overnight fasting of these animals normalised plasma glucose levels and abolished the increased GLUT2 expression (Marks *et al.* 2003). In the present study, we aimed to determine if more subtle changes in plasma glucose concentration may also influence GLUT2 expression at the BBM. Administration of nicotinamide to STZ-injected animals has been shown to partially abolish the diabetogenic effect of STZ and moderate the degree of hyperglycaemia (Masiello *et al.* 1998). Therefore, we adjusted plasma glucose concentrations in STZ-injected animals by using increasing doses of nicotinamide and measured GLUT2 expression at the BBM.

Male Sprague-Dawley rats (250g) received a single i.p. injection of nicotinamide (0, 50, 150 or 200mg/kg) followed by a single tail vein injection of STZ (60mg/kg) 15 min later, administered under light isoflurane anaesthesia. After 2 weeks, rats were terminally anaesthetised, the kidneys removed and the cortex dissected away. BBM vesicles were then prepared at 4°C using the two-stage magnesium precipitation method and GLUT2 expression levels (normalised to β-actin) were established using a standard Western blot protocol. All statistical analyses were performed using ANOVA.

Animals receiving only STZ showed a 2.8-fold increase in plasma glucose concentration (C: 12.1 ± 0.35 vs. STZ: 34.3 ± 1.76 mmol/l, n=6, P<0.001) and a 2.9-fold increase in GLUT2 expression (C: 100% vs. STZ: 292 ± 29%, n=6, P<0.001). Low dose nicotinamide (50mg/kg) reduced plasma glucose levels to 1.85-fold (22.4 ± 3 mmol/l, n=6, P<0.01) and depressed GLUT2 expression to 1.9-fold (192 ± 22%, n=6, P<0.05) of the control values. High dose nicotinamide (200mg/kg) normalised blood glucose (12.4 ± 0.41 mmol/l, n=6) and GLUT2 expression (115 ± 16%, n=6) to levels similar to those found in control animals. Analysis of the results showed a strong correlation ($R^2 = 0.91$) between plasma glucose concentration and GLUT2 expression at the BBM.

We conclude that GLUT2 expression at the proximal tubule BBM is highly dependent on glycaemic status.

Marks J *et al.* (2003). *J Physiol* **553**, 137-145.

Masiello P *et al.* (1998). *Diabetes* **47**, 224-229.

We are grateful to the St Peters Trust of the Middlesex Hospital for financial support.

Where applicable, the authors confirm that the experiments described here conform with the Physiological Society ethical requirements.

PC2

Evidence for P2X receptor-mediated inhibition of sodium reabsorption in collecting ducts from sodium-restricted rats

S.S. Wildman[1], C.M. Turner[1], J. Marks[1], C.M. Peppiatt[1], L.J. Churchill[1], D. Li[2], D.G. Shirley[1], W. Wang[2], B.F. King[1] and R.J. Unwin[1]

[1]Department of Physiology, UCL, London, UK and [2]Department of Pharmacology, New York Medical College, Valhalla, NY, USA

Epithelial sodium channels (ENaC) in the apical membrane of the collecting duct (CD) are co-localised with a variety of ATP-activated P2 receptors. Intraluminal ATP can inhibit ENaC-mediated Na^+ reabsorption (Unwin *et al.* 2003), but there is controversy concerning the P2 receptor subtype responsible. *In vitro* studies in mouse CD implicate the $P2Y_2$ receptor, but *in vivo* studies in the rat suggest otherwise (Shirley *et al.* 2005). Here we have used immunohistochemistry to identify those P2 receptor subtypes present in the apical membrane of the rat CD, and patch-clamp studies to investigate pharmacologically which of these might be responsible for inhibition of ENaC-mediated Na^+ reabsorption.

Kidneys from terminally anaesthetised adult Sprague Dawley rats, that had been maintained on a low (0.01%) sodium diet (in order to increase CD ENaC expression), were perfusion-fixed with paraformaldehyde (4%). Using 8 μm kidney slices from 3 rats and antibodies specific for $P2X_1$-$P2X_7$ receptor subunits and $P2Y_1$, $P2Y_2$, $P2Y_4$, $P2Y_6$, $P2Y_{11}$ and $P2Y_{12}$ receptors, as well as for α-, β- and γ-ENaC subunits, strong immunoflourescence indicated the co-localisation of $P2X_1$, $P2X_2$, $P2X_4$, $P2X_6$ and $P2Y_4$ receptors with ENaC in the CD apical membrane. In further experiments, microdissected CD segments, from rats treated similarly but not perfusion-fixed, were split open to expose the apical membrane of individual principal cells and studied under voltage-clamp conditions using the whole-cell perforated-patch technique. We tested a range of P2 agonists for their activity and for their effect on amiloride (10 μM)-sensitive (i.e. ENaC-mediated) currents. The nucleotides (10 μM) ATP, ATPγS, 2meSATP (all broad-spectrum P2 agonists), Ap_6A ($P2X_1$ selective) and UTP ($P2Y_2$ and $P2Y_4$ selective) all elicited inward currents (amplitude ~500 pA; V_h = -60 mV; n=3). Furthermore, with the exception of UTP, they reduced subsequent amiloride-sensitive current-voltage relationship amplitude (n=3) without changing the inward rectification or reversal potential.

These data are consistent with ionotropic P2X receptor-mediated inhibition of ENaC in the rat CD. Candidate P2X subunits are $P2X_1$, $P2X_2$, $P2X_4$ and/or $P2X_6$.

Unwin RJ *et al.* (2003). *News Physiol Sci* 18, 237-241.

Shirley DG *et al.* (2005). *Am J Physiol Renal Physiol* 288, F1243-1248.

This work was supported by the British Heart Foundation and St Peter's Trust for Kidney, Bladder and Prostate Research.

Where applicable, the authors confirm that the experiments described here conform with the Physiological Society ethical requirements.

PC3

Identification, localization and functional study of epithelial Ca^{2+} channel TRPV6 in the rat epididymis

W. Shum, M. Leung, G. Cheng, S. Au and P.Y. Wong

Physiology, The Chinese University of Hong Kong, Shatin NT, Hong Kong

Calcium is known to play a crucial role in sperm physiology, including motility, metabolism, acrosome reaction, and fertilization. However, very little is known about the regulation of Ca^{2+} in the epididymis, although it is known that the fluid therein has a lower Ca^{2+} concentration than in the blood plasma. The calcium permeable channel TRPV6, but not TRPV5, is expressed in the reproductive tract of male rats as analyzed by RT-PCR and immunohistochemistry. TRPV6 is predominantly present in the apical membranes of the principal cells of the epididymis and the ciliated cells of the efferent duct. Whole-cell patch-clamp studies of isolated epithelial cells from the rat epididymis revealed a Ca^{2+}-selective current with characteristics matching those of the epithelial Ca^{2+} channels, viz constitutive activities, time-dependent inactivation at hyperpolarizing steps of membrane potentials to more negative than –60 mV, inwardly rectifying current-voltage relationship, inhibition by extracellular acidosis but stimulation by alkalosis, and blockade by lanthanum. When the cauda epididymal tubules of anaesthetized rats (pentobarbitone sodium, 60mg kg^{-1}, i.p. injection) were luminally perfused with HCO_3^--buffered Krebs solution (pH_o 7.4) *in vivo*, the perfused segment reabsorbed Ca^{2+} at a rate of 2.6 ± 0.1 nmol cm^{-2} min^{-1} (n=58 from 16 rats). Reabsorption was dose-dependently suppressed by ruthenium red and lanthanum, putative blockers of epithelial Ca^{2+} channels. Castration markedly reduced the Ca^{2+} reabsorptive capacity of the epididymal tubule (n = 16 rats). This study suggests that TRPV6 provides a Ca^{2+} entry pathway that regulates Ca^{2+} homeostasis in the epididymis. Reabsorption of Ca^{2+} by the epididymal tubule is androgen-dependent.

Supported by a grant from the Research Grants Council, Hong Kong.

Where applicable, the authors confirm that the experiments described here conform with the Physiological Society ethical requirements.

PC4

Possible role of apical P2 receptors in modulating aquaporin-2-mediated water reabsorption in the collecting duct

S.S. Wildman[1], C.M. Peppiatt[1], M. Boone[2], I. Konings[2], J. Marks[1], L.J. Churchill[1], C.M. Turner[1], D.G. Shirley[1], B.F. King[1], P.M. Deen[2] and R.J. Unwin[1]

[1]Department of Physiology, UCL, London, UK and [2]Department of Physiology, Radboud University Nijmegen Medical Centre, Nijmegen, Netherlands

Activation of basolateral V_2 receptors by vasopressin increases water reabsorption in the collecting duct (CD) via a series of intracellular events that culminate in increased insertion of aquaporin-2 water channels (AQP2) into the apical membrane. Recent studies have shown that this process is inhibited by extracellular ATP acting on P2 receptors expressed on the basolateral membrane of CD principal cells, and that $P2Y_2$-like receptors are responsible (Unwin *et al.* 2003). The present study has used the *Xenopus* oocyte expression system to investigate whether other P2 receptor subtypes can influence AQP2 function, and has localised P2 receptor distribution in the rat CD.

Defolliculated *Xenopus* oocytes (co-expressing AQP2 and a given P2 receptor) were placed in a hypotonic (10 mosm/l) Barth's solution, and AQP2-mediated swelling was monitored by video imaging at 1.7 s intervals for 1 min; from this, osmotic water permeability (P_f) was calculated (Deen *et al.* 1994). When $P2X_2$, $P2Y_2$ or $P2Y_4$ receptors were co-expressed with AQP2, then activated by 10 μM ATP, P_f was reduced significantly (by $46 \pm 8\%$ ($P<0.01$, unpaired *t* test), $53 \pm 7\%$ ($P<0.01$) and $57 \pm 3\%$ ($P<0.01$), respectively; means ± SEM; $n=8$ in each case). Western blot analysis, with a specific AQP2 antibody, confirmed that the P2 receptor-mediated inhibition of cell swelling was due to removal of AQP2 protein from the plasma membrane in each case ($n=3$).

Kidneys from three terminally anaesthetised adult Sprague Dawley rats were perfusion-fixed with paraformaldehyde (4%) and sliced (8 μm). Using antibodies specific for $P2X_2$, $P2Y_2$ and $P2Y_4$ receptors, immunohistochemical analysis demonstrated the expression of $P2X_2$ and $P2Y_4$ receptors on the apical membrane throughout the CD and $P2Y_2$ on the basolateral membrane in the inner medullary CD.

These results show directly that activation of certain P2 receptors can inhibit AQP2-mediated water transport. They also suggest that, in addition to the previously documented effect of basolateral $P2Y_2$ receptors, apically located P2 receptors ($P2X_2$ or $P2Y_4$) might play a role in modulating vasopressin-stimulated water reabsorption in the CD, thus strengthening suggestions that intraluminal nucleotides might act as paracrine/autocrine agents.

Unwin RJ *et al.* (2003). *News Physiol Sci* 18, 237-241.

Deen PMT *et al.* (1994). *Science* 264, 92-95.

This work was supported by the British Heart Foundation and St Peter's Trust for Kidney, Bladder and Prostate Research.

Where applicable, the authors confirm that the experiments described here conform with the Physiological Society ethical requirements.

PC5

Acute regulation of the urea transporter UT-A3, expressed in a MDCK cell line

G.S. Stewart, E. Potter and C. Smith

Faculty of Life Sciences, The University of Manchester, Manchester, UK

Renal facilitative urea transporters play a vital role in the urinary concentrating mechanism (Fenton *et al.* 2004). UT-A3 is a phloretin-sensitive urea transporter expressed on the basolateral membrane of inner medullary collecting duct cells (Stewart *et al.* 2004). In this study, we have produced a MDCK cell line that stably expresses myc-tagged UT-A3, and investigated the resulting urea transport in these MDCK:UT-A3 cells. Radioactive ^{14}C-

labelled urea flux experiments showed that during basal conditions there was no difference in basolateral urea uptake into control MDCK cells (1.72 ± 0.22 nmol cm^{-2} min^{-1}, n=16) and MDCK:UT-A3 cells (1.99 ± 0.24 nmol cm^{-2} min^{-1}, n=16) (NS, unpaired t test). However, while pre-incubation for 60 min in 10^{-6} M arginine vasopressin (AVP) had no effect on urea uptake into control MDCK cells (1.94 ± 0.09 nmol cm^{-2} min^{-1}, n=4, NS, ANOVA), it significantly stimulated urea uptake into MDCK:UT-A3 cells (6.12 ± 0.68 nmol cm^{-2} min^{-1}, n=4, $P<0.05$, ANOVA); as did 60 min pre-incubation with 10^{-6} M AVP (5.23 ± 0.66 nmol cm^{-2} min^{-1}, n=4, $P<0.05$, ANOVA). Further investigation showed that this 10^{-6} M AVP response was in fact biphasic, with an initial peak after 10 min (5.31 ± 0.70 nmol cm^{-2} min^{-1}, n=4, $P<0.05$, ANOVA) followed by a larger response after 60 min (7.07 ± 0.74 nmol cm^{-2} min^{-1}, n=4, $P<0.05$, ANOVA). Importantly, the 60 min AVP response was significantly inhibited by 500 μM phloretin (73 ± 8% of control, n=4, $P<0.05$, ANOVA). Finally, MDCK:UT-A3 urea uptake was also stimulated by 10 μM forskolin (5.53 ± 0.78 nmol cm^{-2} min^{-1}, n=4, $P<0.01$, ANOVA), 250 μM 8-bromo-cAMP (3.74 ± 0.23 nmol cm^{-2} min^{-1}, n=4, $P<0.05$, ANOVA) or 1 mM ATP (4.73 ± 0.56 nmol cm^{-2} min^{-1}, n=4, $P<0.05$, ANOVA). In conclusion, our results indicate that phloretin-sensitive UT-A3 urea transport can be regulated by AVP, possibly via intracellular increases of cAMP and/or calcium.

Fenton RA *et al.* (2004). *Proc Natl Acad Sci* **101**, 7469-7474.

Stewart GS *et al.* (2004). *Am J Physiol Renal* **286**, F979-F987.

This work was funded by Kidney Reseach UK.

Where applicable, the authors confirm that the experiments described here conform with the Physiological Society ethical requirements.

PC6

A new role for a famous gene: *white* encodes a *Drosphila* renal cyclic GMP transporter

J.M. Evans, J.P. Day, S.A. Davies and J.A. Dow

Molecular Genetics, University of Glasgow, Glasgow, UK

Drosophila Malpighian (renal) tubules are a powerful and adaptable model for studying *in vitro* epithelial transport mechanisms. Mutations in the *white* gene were the very first identified by Morgan. *White* is one of the most important genetic markers in modern *Drosophila* molecular biology; however, its function is surprisingly poorly understood. Previous studies have shown that *white* gene encodes a member of the G family [1] of ATP binding cassette (ABC) transporters, and is implicated in the transport of kynurenine, tryptophan and guanine. However, the function of *white* is surprisingly poorly understood considering it is one of the most important markers in modern *Drosophila* molecular biology. Cyclic guanosine 3',5'-cyclic monophosphate (cGMP) is a signalling molecule involved in the regulation of a diverse range of tissues [2]. Cyclic GMP can be actively transported by various ABC transporters [3].

In a recent Affymetrix microarray experiment *white* was found to be 10.3 ± 1.4 (mean ± SEM, N=5) up-regulated in the Malpighian tubules [4] and differentially expressed when the tubules were incubated with cGMP. As the tubules are stimulated by exogenous cGMP, and are known to transport cyclic nucleotides, we hypothesised that *white* might be involved in cGMP transport. Using ^3H labelled cGMP in a transport assay [5], wild-type tubules were shown to transport cGMP at a rate of 2.22 ± 0.24 fmol min^{-1} (mean ± SEM, N=19), while in *white* mutant the rate of transport was 0.86 ± 0.09 fmol min^{-1} (mean ± SEM, N=18), significantly ($P<0.001$) less cGMP than wild type tubules. A number of pharmaceutical competitors effect on cGMP transport were characterized, including glibenclamide, methotrexate, kynurenine, and tryptophan. Interestingly cAMP does not compete with cGMP transport, suggesting that the transport of these cyclic nucleotides is independent in *Drosophila* renal tubules. The *white* protein appears to be expressed at the basolateral membrane, using ICCs and a GFP-labelled overexpression construct. Further secretion assays demonstrate that even in the presence of cGMP transport inhibitors, or in *white* mutants, cGMP stimulates fluid secretion by tubules, suggesting an independent receptor-mediated action of cGMP, that does not require transepithelial transport.

Dean M, Rzhetsky A & Allikmets R (2001). In ABC Proteins from Bacteria to Man, 1st edn, pp. 47-61. Academic Press, London.

Davies SA (2006). Cell Signal 18, 409-421.

Sager G (2004). Neurochem Int 45, 865-873.

Wang J, Kean L, Yang J, Allan AK, Davies SA, Herzyk P & Dow JA (2004). Genome Biol 5, R69.

Evans JM, Allan AK, Davies SA & Dow JA (2005). J Exp Biol 208, 3771-3783.

This work is funded by the Biotechnology and Biological Sciences Research Council.

Where applicable, the authors confirm that the experiments described here conform with the Physiological Society ethical requirements.

PC7

Immunohistochemical localisation of P2 receptors in the rat renal collecting duct: effects of altering dietary sodium intake

E. Chapman, S. Hussain, C.M. Peppiatt, J. Marks, L.J. Churchill, C.M. Turner, B.F. King, R.J. Unwin and S.S. Wildman

Department of Physiology, UCL, London, UK

ATP can be detected in urine at concentrations sufficient to activate P2 receptors (P2Rs) expressed in the luminal membrane of renal tubular cells (Unwin *et al.* 2003). The activation of certain apical P2Rs by extracellular ATP has been shown to inhibit Na^+ transport in the collecting duct (CD) *in vitro* and *in vivo*. Previously, using the *Xenopus* oocyte expression system, we have demonstrated a regulatory interdependence between certain P2Rs and the epithelial Na^+ channel (ENaC) (Wildman *et al.* 2005). We have shown that plasma membrane expression of P2R assemblies incorporating $P2X_2$, $P2X_5$ and $P2X_6$ subunits are directly increased by ENaC expression and that ENaC activity is decreased by the stimulation of P2R assemblies incorporating $P2X_2$, $P2X_4$ and $P2X_6$ subunits. We have proposed that some P2Rs may provide localised and fine regulation of ENaC activity in the CD *in vivo*.

Kidneys from terminally anaesthetised adult Sprague Dawley rats (maintained on low (0.01%), normal (0.5%) or high (4%)

sodium diets, for 10 days) were perfusion-fixed with paraformaldehyde (4%) and sliced (8 μm). We used co-immunofluorescence (using an AQP2 antibody as a marker of the CD) to investigate apical P2R expression patterns along the CD in response to changes in dietary sodium intake (that also change ENaC expression).

In rats maintained on a normal Na^+ diet (n=3), immunostaining for $P2X_4$ and $P2X_6$ ion channel receptor subunits and $P2Y_4$, $P2Y_6$, $P2Y_{11}$ and $P2Y_{12}$ metabotropic receptors was evident in the apical membrane throughout the CD. Weak staining was seen for apical $P2X_2$, $P2X_5$ and $P2X_7$ receptors. In rats on a low Na^+ diet (n=3), expression of $P2X_1$ also became apparent, expression of $P2X_2$ was increased and immunostaining for $P2X_5$ disappeared. With the exception of $P2Y_4$, all previously detected P2Y receptors showed restricted co-localisation and weak apical staining. A high Na^+ diet also resulted in increased apical expression of $P2X_1$, but in contrast to normal and low Na^+ diets expression of apical $P2X_7$ receptors was increased and immunostaining for $P2X_2$ disappeared. We also saw weak staining for those P2Y receptors previously detected in abundance, with exception of $P2Y_6$ and $P2Y_{12}$, which remained unchanged.

In summary, apical P2R expression patterns change in the rat CD in response to changes in dietary sodium intake. Our results support a link between P2R expression and function and ENaC regulation (i.e. assemblies of $P2X_2$, $P2X_4$ and $P2X_6$ subunits, having the ability to inhibit ENaC activity, shown here to mirror ENaC expression *in vivo*), which, itself, is regulated by levels of dietary Na^+.

Unwin RJ *et al.* (2003). *News Physiol Sci* 18, 237-241.

Wildman SS *et al.* (2005). *J Am Soc Nephrol* 16, 2586-2597.

E.C. and S.H. contributed equally to this work.

This work was supported by the British Heart Foundation and St Peter's Trust for Kidney, Bladder and Prostate Research.

Where applicable, the authors confirm that the experiments described here conform with the Physiological Society ethical requirements.

PC8

A Ca^{2+}-activated Cl^- conductance supports the regulatory volume decrease of mouse renal collecting duct cells in primary culture

S.H. Boese

Zoophysiology, University of Potsdam, Golm, Brandenburg, Germany

Cells of the renal inner medullary collecting duct (IMCD) are able to regulate their volume after hypoosmotic perturbations (regulatory volume decrease, RVD) by activating a swelling-sensitive anion/organic osmolyte channel (VRAC) [1]. As full activation of VRAC takes several minutes it might be of advantage for the IMCD cells to recruit other anion conductances for support, especially in case of massive hypoosmotic stress. A possible candidate might be the Ca^{2+}-activated Cl^- conductance (CaCC), as it can be recruited rapidly by even a small increase in intracellular calcium ($[Ca^{2+}]_{in}$) [2].

To investigate this hypothesis, cells isolated from the initial third of the mouse IMCD (mIMCD; see [2]) were cultured on glass coverslips (Media osmolality: 600 mosmol/kg H_2O) and challenged with either a moderate (bath osmolality reduction by 100 mosmol/kg H_2O via removal of sucrose) or a massive (bath osmolality reduction by 300 mosmol/kg H_2O via removal of sucrose) hypoosmotic shock, respectively. Membrane conductance changes of the cells were investigated using the slow whole cell patch-clamp technique (Nystatin perforated patch). Currents were attributed to VRAC or CaCC by their distinct biophysical characteristics (see [1]). Alterations in $[Ca^{2+}]_{in}$ were measured by intracellular ratiometric Ca^{2+} imaging using the fluorescent calcium indicator Fura2. Data are given as mean±SEM (n), statistical significance was tested as in [1].

A moderate hypoosmotic challenge via a reduction of the extracellular osmolality by 100 mosmol/kg H_2O resulted in activation of VRAC. However, neither a significant increase in $[Ca^{2+}]_{in}$ nor an activation of CaCC was detectable.

On the other hand, challenging the mIMCD cells with a massive hypoosmotic shock (-300 mosmol/kg H_2O) elicited not only VRAC activity but also an increase in $[Ca^{2+}]_{in}$ in conjunction with activation of CaCC. $[Ca^{2+}]_{in}$ rose from a basal level of 28±5nM (n=7) to 367±21nM (n=7), and membrane conductance grew from -2.4±0.8pA/pF to -12.2±1.2pA/pF at -80mV and from 4.2±0.9pA/pF to 72±2.1pA/pF at +80mV (n=11), respectively. The increase in $[Ca^{2+}]_{in}$ could be detected 31±5s (n=10) after the start of the hypoosmotic challenge and lasted as long as the osmotic gradient was maintained.

Omission of calcium in the extracellular bathing solution ($[Ca^{2+}]_{ex} < 10$nM) had neither a significant effect on the intracellular Ca^{2+} signal nor on the CaCC activity elicited by the hypoosmotic challenge. Chelation of intracellular Ca^{2+} on the other hand prevented the $[Ca^{2+}]$in rise as well as CaCC activation. This indicates intracellular calcium stores as the main Ca^{2+} source for the signal.

In conclusion, activation of CaCC via an intracellular calcium signal seems to support the RVD of mIMCD cells after a strong hypoosmotic challenge by providing an early anion efflux pathway which precedes the slower activating VRAC conductance.

Boese SH *et al.* (2000). *J Mem Biol*, **177**, 51-64.

Boese SH *et al.* (2004). *Am J Physiol*, **286**, F682–F692.

Where applicable, the authors confirm that the experiments described here conform with the Physiological Society ethical requirements.

PC9

17β-Oestradiol rapidly activates intracellular calcium signalling via a protein kinase C—protein kinase A-dependent pathway in the human eccrine sweat gland cell line NCL-SG3

R.W. Muchekehu, A. Hartford and B.J. Harvey

Molecular Medicine, Royal College of Surgeons in Ireland, Dublin, Ireland

β-Adrenergic-stimulated sweat secretion is mediated by calcium and cAMP. We describe here, for the first time, protein kinase A- (PKA) and protein kinase C- (PKC) dependent modulation of intracellular calcium ($[Ca^{2+}]_i$) by the hormone 17 β-oestra-

diol (E_2) in the human eccrine sweat gland cell line NCL-SG3. We have previously shown that E_2 rapidly activates PKC isoforms and PKA in NCL-SG3 cells (1).

Changes in $[Ca^{2+}]_i$ were measured using ratiometric fluorescence microscopy on cells loaded with Fura 2-AM. Variations in $[Ca^{2+}]_i$ are expressed as ratios of fluorescent intensities F(t)/F(t0) where F(t) refers to the Fura 2 fluorescence intensity at a given time (t) and F(t0) to fluorescence intensity at zero time basal levels.

Cells treated with thapsigargin responded with a transient single spike-like increase in calcium, which then returned to zero time basal levels. Exposure of cells to both E_2 and thapsigargin produced a secondary, sustained increase in $[Ca^{2+}]_i$ ($F(t20)/F(t0) = 2.68 \pm 0.15$; n=8 compared with thapsigargin treatment alone, $F(t20)/F(t0) = 1$; n=8). This effect was independent of extracellular calcium and is specific to 17β oestradiol, as 17α oestradiol and testosterone had no effect on $[Ca^{2+}]_i$.

The E_2-induced increase in $[Ca^{2+}]_i$ was abolished by the PKC inhibitor chelerythrine chloride (1μM), by the PKA inhibitor Rp-adenosine 3',5'-cyclic monophosphorothioate (200μM), and by the adenylyl cyclase inhibitor SQ22536 (200μM). Xestospongin C (10μM), a membrane-permeable selective inhibitor of IP_3-induced Ca^{2+} release and IP_3 receptor-mediated signalling, failed to abolish the E_2-induced increase in $[Ca^{2+}]_i$. However, ryanodine (100μM), which at high concentrations is an established inhibitor of ryanodine receptors, completely abolished the E_2-induced increase in $[Ca^{2+}]_i$.

These results demonstrate a novel mechanism by which E_2 modulates $[Ca^{2+}]_i$ via a PKC-PKA-dependent pathway from intracellular Ca^{2+} stores regulated through ryanodine receptors.

Muchekehu RW et al. (2004). *J Physiol* **557P**, PC96.

This work is funded by the Higher Education Authority in Ireland (PRTLI Programme) and UNILEVER plc.

Where applicable, the authors confirm that the experiments described here conform with the Physiological Society ethical requirements.

PC10

Localisation of transport proteins in the syncytiotrophoblast from first trimester and term human placenta

K. Mynett, P.F. Speake, J. Glazier, S. Greenwood, H. Lacey and C. Sibley

Division of Human Development, University of Manchester, Manchester, UK

The human placenta shows marked developmental changes over the course of pregnancy and previous data suggest that the transport function of the syncytiotrophoblast also changes from first trimester to term. Directional transport of solutes across the placenta depends on asymmetric distribution of transporter proteins in the maternal facing microvillous (MVM) and the fetal facing basal (BM) plasma membrane of the syncytiotrophoblast. It is evident that some solute transport proteins show polarised localisation to the MVM or BM at term, but little is known about the development of polarity throughout gestation. The localisation to MVM and BM of several transport proteins (plasma membrane Ca^{2+}-ATPase PMCA, GLUT1, Na^+-H^+ exchanger NHE1, transferrin) in term (T) and first trimester (FT) placenta was assessed by immunohistochemistry.

Fragments of placental villi were randomly sampled from FT (6-12 weeks; n=4) and T (n=3 or 4) placentas and immediately preserved in zinc fixative (Johannson et al. 2000). Villi were paraffin embedded, sectioned, incubated with primary then biotinylated secondary antibodies and counterstained with methyl green. Six sections were imaged for each placenta and assessed by three independent observers, blind to antibody and gestation. For each placenta, the mean of the observer scores for each antibody was calculated to achieve an average for each placenta. The values are expressed as mean±SEM with n = number of placentas.

All the transport proteins investigated were detected in both MVM and BM in both FT and T tissue. Transferrin showed more staining localized to the MVM compared to the BM in both FT (0.93±0.07 compared to 0.26±0.11) and T (1.0±0.01 compared to 0.32±0.13). PMCA (MVM 0.88±0.11 compared to BM 0.90±0.09) and NHE 1 (MVM 0.93±0.04 compared to BM 0.81±0.13) showed equal distribution to the MVM and the BM in FT. At term, PMCA (MVM 0.19±0.10 compared to BM 0.98±0.019) and NHE 1 (MVM 0.65±0.01 compared to BM 1.00±0.01) showed a more polarised distribution to the BM. GLUT1 was expressed equally in the MVM and BM at both FT (MVM 0.74±0.14 compared to BM 0.75±0.15) and T (MVM, 0.75±0.10 compared to BM 0.94±0.02).

In conclusion, the non polarised distribution of GLUT1 and the polarised distribution of transferrin was maintained throughout gestation. There was a maturation of the distribution of PMCA and NHE1 from expression on both MVM and BM in FT to predominantly BM at T. The term distribution of NHE1 and PMCA predominantly to BM is consistent with previous reports (Speake et al. 2005). The maturation of distribution of these transporters may have functional implications for ion transport across the placenta during gestation highlighting the need for studies on the mechanisms of transporter trafficking in the human placenta.

Johansson et al. (2000). Am J Physiol 279, R287-R294.

Speake et al. (2005). Pflugers Arch 450, 123-130.

Supported by The Wellcome Trust.

Where applicable, the authors confirm that the experiments described here conform with the Physiological Society ethical requirements.

PC11

Induction of Na^+-K^+-$2Cl^-$ co-transporter expression mediates chronic potentiation of intestinal Cl^- secretion by epidermal growth factor

F. O'Mahony and S.J. Keely

Molecular Medicine, Royal College of Surgeons in Ireland, Dublin, Ireland

Epidermal growth factor (EGF) is well known to promote intestinal epithelial barrier function [1]. However, its role in regulating epithelial transport function is less well understood. We have previously shown that acute treatment with EGF chronically enhances epithelial responsiveness to both Ca^{2+} and cAMP-dependent secretagogues. Here, we investigated the molecular mechanisms involved. T_{84} colonic epithelial cells were grown as polarized monolayers on permeable supports. Changes in I_{sc}, indicative of electrogenic ion transport, were measured by the Ussing chamber/voltage clamp technique. Protein and mRNA

expression were measured by Western blotting and PCR, respectively. Intracellular Ca^{2+} ($[Ca^{2+}i]$) was measured by Fura-2 fluorescence and protein kinase A (PKA) activity with the Promega PepTag assay kit. Acute treatment of T_{84} cells with EGF (100 ng/ml; 15 min) chronically enhanced subsequent I_{sc} responses to the Ca^{2+}-dependent agonist, carbachol (CCh, 100 μM). This effect was only apparent after 3 h and was maximal by 6 h after stimulation with EGF at which time responses to CCh were 206.1 ± 28.3% of those in control cells (n = 4; p< 0.01). The potentiating effect of EGF was sustained for at least 24 h. The Na^+-K^+-$2Cl^-$ co-transporter (NKCC1) inhibitor, bumetanide (100 μM), abolished the effect of EGF, indicating Cl^- secretion to be involved. Neither basal nor agonist-stimulated levels of intracellular Ca^{2+} or PKA activity were altered by EGF pretreatment, implying the effects of the growth factor are not due to chronic alterations in levels of second messengers. Western blot analysis revealed that EGF increased the expression of NKCC1 with a time course that closely paralleled its effects on Cl^- secretion. This effect of EGF was maximal after 6 h, at which time NKCC1 expression in EGF-treated cells was 199.9 ± 21.9% of that in control cells (n =21; p<0.0001). EGF also increased the CFTR expression (by 3.9 ± 1.1-fold; n=5; p<0.01) but not that of the Na^+/K^+ ATPase pump. EGF-induced NKCC1 expression was abolished by the inhibitor of transcription, actinomycin D, implying EGF upregulates NKCC1 expression at the level of gene transcription. Finally, rtPCR analysis showed that within 1–4 h after stimulation with the growth factor, EGF increased expression of NKCC1 mRNA to levels that were 160 ± 11.9% of those in control cells (n=3; p<0.05). These data reveal a novel role for EGF in chronically regulating epithelial secretion at the fundamental level of transport protein expression. EGF enhances epithelial secretory capacity by inducing NKCC1 expression, an effect which in vivo would serve to promote epithelial hydration, thereby enhancing barrier function. These data suggest that further elucidation of EGF-dependent signalling pathways may yield new targets for drug development in treatment of intestinal transport disorders.

Basuroy S, Sheth P, Mansbach CM & Rao RK (2005). Am J Physiol 289, G367-G375.

Where applicable, the authors confirm that the experiments described here conform with the Physiological Society ethical requirements.

PC12

Adenosine induces Na^+ absorption in a human bronchiolar epithelial (H441) cell line

M. Constable, S.K. Inglis, L.A. Chambers, R.E. Olver and S.M. Wilson

Maternal and Child Health Sciences, University of Dundee, Dundee, UK

Previous studies show activation of $P2Y_2$ receptors by UTP inhibits Na^+ absorption in airway epithelial cells (Inglis et al. 1999, 2000; Ramminger et al. 1999) which may provide a method to control the Na^+ hyper-absorption which occurs in the lungs of cystic fibrosis patients.

Preliminary studies in H441 cells show UTP inhibits, whereas ATP unexpectedly stimulates Na^+ absorption. As $P2Y_2$ receptors are equally sensitive to both, there must be another receptor which underlies the effects of ATP. Further experiments suggested the non $P2Y_2$ mediated response of ATP may be a result of ATP hydrolysis resulting in the stimulation of adenosine receptors. The aim of this study was to investigate the pharmacological basis of the effect of adenosine in H441 cells.

H441 cells were grown on Costar snapwells in RPMI-1640 media supplemented with dialysed FBS and 0.2μM dexamethasone. Once confluent, cells were mounted onto Ussing chambers, bathed in physiological saline and gassed with 13% O_2 at 37°C.

Basal values of potential difference, short circuit current (I_{sc}) and transepithelial resistance were 11.7±1.1mV, 44.6±3.3μAcm^{-2} and 257.8±5.7Ωcm^2, respectively (n=240). Apical adenosine (200μM) evoked a slow increase in I_{sc} (60.54±.5μA cm^{-2}) compared to pre-stimulated I_{sc} (39.5±4.5μA cm^{-2}, n=8, p<0.05). This increase in I_{sc} is associated with an increase in apical sodium conductance (G_{Na}), stimulated cells (354.9±41.3μS cm^{-2}) *vs.* control cells (213.5±36.5μS cm^{-2}, n=6, p<0.001).

To establish which adenosine receptor mediates the response, cells were subjected to a range of adenosine agonists and antagonists. Concentration curves for adenosine and three adenosine receptor agonists, SPA (A1), CGS 21680 ($A2_A$) and IB-MECA (A3) were constructed. From these curves the EC_{50} was calculated, adenosine 1.6±0.7μM, SPA 1.5±0.3μM, CGS 21680 8.4±0.9μM and IB-MECA 6.2±1.5μM, therefore rank order of potency is adenosine ≈ SPA > CGS 21680 ≈ IB-MECA. As none of these agonists are more potent than adenosine it may be that the adenosine response is mediated by $A2_B$ receptors, however this is difficult to confirm as there are no commercially available $A2_B$ receptor agonists.

We therefore investigated the effects of adenosine receptor antagonists (DPCPX (A1), ZM 241385 ($A2_A$) and MRS 1706 ($A2_B$)) on I_{sc} of cells pre-stimulated with maximal adenosine. DPCPX had no effect, whereas ZM241385 and MRS1706 both appear to displace adenosine from its receptor, although the effects of these two antagonists are indistinguishable.

These data suggest a role for $A2_A$ and/or $A2_B$ receptors in the stimulation of Na^+ absorption in response to apical adenosine in H441 cells.

Inglis SK, Collett A, McAlroy HL, Wilson SM & Olver RE (1999). Pflügers Archiv 438, 621-627.

Inglis SK, Olver RE & Wilson SM (2000). Br J Pharmacol 180, 367-374.

Ramminger SJ, Collett A, Baines DL, Murphie H, McAlroy HL, Olver RE, Inglis SK & Wilson SM (1999). Br J Pharmacol 128, 293-300.

This project was funded by the Wellcome Trust.

Where applicable, the authors confirm that the experiments described here conform with the Physiological Society ethical requirements.

PC13

Insulin stimulates Na^+ transport in H441 human distal lung epithelial cells

E.M. Husband, S.K. Inglis, R.E. Olver and S.M. Wilson

Maternal and Child Health Sciences, University of Dundee, Dundee, UK

Insulin treatment improves alveolar-capillary gas exchange in type 2 diabetes, one suggested mechanism being insulin-evoked

stimulation of alveolar epithelial fluid absorption [1]. Studies in A6 (*Xenopus* renal epithelial) cells [e.g. 2] have shown that insulin can stimulate epithelial Na^+ transport, in turn providing an osmotic driving force for increased fluid absorption. There is however little data regarding the effect of insulin on lung epithelial Na^+ transport and hence this study aims to investigate the response to insulin in H441 distal lung epithelial cells.

H441 cells were grown on permeable supports and after 8 days resistive monolayers were mounted in Ussing chambers. Data are mean ± S.E.M. analysed by Student's paired t test (significant if $P<0.05$).

In this laboratory, H441 cells are routinely cultured in the presence of insulin (0.87 μM) and so the effect of removing it from the culture medium was assessed. Indeed cells grown in the absence of insulin displayed altered basal properties relative to age-matched cells grown in its presence. The removal of insulin resulted in decreased potential difference from 8.43 ± 0.96 to 3.02 ± 0.51 mV (n=6, $P<0.001$), short circuit current (I_{sc}) was also reduced from 25.88 ± 3.49 to 14.59 ± 2.16 μA cm^{-2} (n=6, $P<0.001$) and transepithelial resistance (R_t) fell from 321.83 ± 33.05 to 199.67 ± 9.18 Ω cm^{-2} (n=6, $P=0.019$).

As a result of these findings we investigated the effect of acute addition of insulin to cells cultured in its absence. 20nM (sufficient to stimulate Na^+ transport in A6 cells [(2)]) was added to the basolateral membrane under short circuit conditions and evoked an increase in I_{sc} of ~40% (13.23 ± 1.55 to 18.38 ± 1.97 μA cm^{-2}, n=6, $P<0001$). Studies in basolaterally permeabilised cells showed that the amiloride-sensitive apical Na^+ conductance was also increased by 20 nM insulin (74.86 ± 14.87 μS cm^{-2} vs control 51.46 ± 10.56 μS cm^{-2}, n=5, $P=0.013$) confirming the changes in I_{sc} represent increased Na^+ influx through the apical membrane.

Insulin-evoked Na^+ transport in A6 cells is dependent on the activity of PI-3-Kinase [2]. Likewise in the present study the PI-3-Kinase inhibitor LY-294002 (LY) inhibited both basal and insulin-stimulated I_{sc}. Basal I_{sc} was reduced by ~65% (from 14.90 ± 1.35 to 4.99 ± 0.56 μA cm^{-2}) while the response to insulin was all but abolished (increase in I_{sc} of only 0.23 ± 0.17 μA cm^{-2} after LY vs control response of 5.66 ± 0.76 μA cm^{-2}). Interestingly, previous experiments have shown LY had no effect on the stimulatory response to forskolin addition in H441 cells [3], indicating a distinction between the signalling pathways used by these two agents to stimulate Na^+ transport.

In summary insulin stimulates Na^+ transport in human H441 lung cells, at least in part by increasing apical Na^+ conductance. This response appears to be mediated via PI-3-Kinase.

Guazzi M *et al.* (2002). Diabetes Care **25**, 1802-1806.

Record RD *et al.* (1998). Am J Physiol **274**, E611-617.

Husband EM *et al.* (2005). J Physiol **565P** PC36.

This work was supported by the Wellcome Trust and The George John Livanos Trust.

Where applicable, the authors confirm that the experiments described here conform with the Physiological Society ethical requirements.

PC14

Basolateral K^+ conductance in a human airway epithelial cell line

S.K. Inglis and S.M. Wilson

Maternal and Child Health Sciences, University of Dundee, Dundee, UK

The luminal surface of the airways is covered with the airway surface liquid (ASL), which plays an important role in host pulmonary defence. To fulfil this role its volume and composition must be controlled, and this is achieved through the regulation of ion, and hence liquid, transport across the epithelium. At rest, the airway epithelium is primarily absorptive. Na^+ is absorbed from the ASL through apical Na^+ channels (ENaC), and pumped across the basolateral membrane by Na^+/K^+ATPase. To maintain the electrochemical driving force for this process, basolateral K^+ conductances (G_K) enable K^+ efflux. Whilst a great deal is known about the control of ENaC, relatively little is known about the nature and regulation of G_K. The aim of this study was to investigate the basolateral G_K present in the human bronchiolar cell line, H441.

H441 cells were grown to confluence on permeable supports (2) and mounted in Ussing chambers containing HCO_3^--buffered Kreb's solution. Transepithelial PD was monitored (voltage clamp; WPI) and recorded directly to computer using a Powerlab interface (ADInstruments). Once PD was stable (20min), the bathing solutions were replaced with solutions modified to impose an apical (135mM K^+) to basolateral (4.7mM K^+) K^+ gradient and a maximal dose of amphotericin B was added (200μM). PD rose to a new, stable level (7.3±0.3 to 12.2±0.5mV, n=50) and then monolayers were short circuited. Ba^{2+} (5mM), clofilium (100μM) and clotrimazole (100μM) inhibited 52±10%, 76±15% and -6±4% of amphotericinB-induced I_K, respectively. 1-Ethyl-2-benzimidazolinone (EBIO, 1mM), an activator of Ca^{2+}-activated K^+ channels (1) increased I_K by 20.2±3.6μA cm^{-2} (n=8). However, this was unaffected by a blocker of EBIO-sensitive $K_{Ca}3.1$ channels, clotrimazole. Unexpectedly, thapsigargin (1μM) had no effect on I_K. ATP (100μM) evoked a transient increase (21.0±1.9μA cm^{-2}, n=9) that was unaffected by either clofilium, Ba^{2+} or clotrimazole but inhibited by clamping PD at the K^+ equilibrium potential (E_K, -89mV). Both adenosine (200μM) and forskolin (10μM) evoked small increases in I_K (3.4±2.0, n=6 and 5.4±1.6, n=4, respectively).

H441 cells possess basolateral G_K that are regulated by a number of agonists known to control transepithelial Na^+ transport, and include both those that alter intracellular Ca^{2+} concentration (ATP), and those controlling cAMP levels (forskolin and adenosine). The lack of a response to thapsigargin may indicate that G_K is regulated by transient increases in intracellular Ca^{2+} as evoked by ATP, rather than the bulk changes in cytoplasmic Ca^+ levels induced by thapsigargin. Alternatively, ATP may exert its effect by some other, as yet unknown, action. Since clotrimazole had no effect on either basal I_K or following stimulation with EBIO, $K_{Ca}3.1$ channels are unlikely to underlie basolateral G_K in these cells.

Devor DC, Singh AK, Lambert LC, DeLuca A, Frizzell RA & Bridges RJ (1999). J Gen Physiol 113, 743-760.

Ramminger SJ, Richard K, Inglis SK, Land SC, Olver RE & Wilson SM (2004). Am J Physiol 287, L411-L419.

Supported by The Wellcome Trust (SKI Project grant).

Where applicable, the authors confirm that the experiments described here conform with the Physiological Society ethical requirements.

PC15

NKCC1 does not contribute to volume regulation in epithelial cells isolated from mouse choroid plexus

P.D. Brown, A. Pakhomova and I.D. Millar

Faculty of Life Sciences, University of Manchester, Manchester, M13 9PT, UK

NKCC1 is highly expressed in the apical membrane of choroid plexus epithelial cells (Wu et al. 1998). It is not known, however, whether the transporter mediates the influx (Wu et al. 1998) or efflux of ions (Keep et al. 1994). In this study we have investigated the possible role of NKCC1 in the regulation of cell volume.

The choroid plexus was dissected post mortem from the fourth ventricle of mice. Epithelial cells were isolated using dispase and cell volume measured by a video-imaging method.

Wu et al. (1998) concluded that NKCC1 mediates ion influx based largely on the observation that 100 μM bumetanide caused a decrease in cell volume in isotonic solutions. A similar effect of 100 μM bumetanide was observed in 3 cells in this study; however, 10 μM bumetanide (a dose sufficient to inhibit NKCC1) had no effect on cell volume in isotonic solutions (n=7). The effect of 100 μM bumetanide on volume may therefore be due to non-specific effects of the drug.

When exposed to hypertonic solutions cells immediately shrank as expected. In HEPES-buffered solutions a volume recovery was not observed (n=4). By contrast in HCO_3^--buffered solutions a substantial regulatory volume increase (RVI) was observed (n=7). Neither 10 μM (n=5) nor 100 μM bumetanide inhibited this RVI (n=5). The RVI, however, was almost completely abolished four experiments by 10 μM methyl-isobutyl amiloride (an inhibitor of NHE; $P< 0.05$ by unpaired t test compared to control). These data indicate that NHE (probably coupled to AE) and not NKCC1 are responsible for the RVI in choroid plexus epithelial cells.

In conclusion, NKCC1 does not appear to have a role in maintaining the volume of choroid plexus epithelial cells. The contribution of NKCC1 to ion fluxes in choroid plexus cells therefore remains to be established.

Keep RF, Xiang J & Betz AL (1994). *Am J Physiol* **267**, C1616-1622.

Wu Q, Delpire E, Hebert SC & Strange K (1998). *Am J Physiol***275**,C1565-C1572.

Supported by the Wellcome Trust.

Where applicable, the authors confirm that the experiments described here conform with the Physiological Society ethical requirements.

PC16

Characterisation of a non-selective cation channel in mouse choroid plexus epithelial cells

I. Millar and P. Brown

Faculty of Life Sciences, University of Manchester, Manchester, UK

Transient receptor potential (TRP) ion channels comprise a newly identified family of cation-permeable channels (Nilius & Voets, 2005). Here we detail evidence that choroid plexus exhibits a non-selective cation channel with similarities to TRP channels.

Fourth ventricle choroid plexus were isolated post mortem from mice. Cellular currents were determined by whole cell patch clamp on intact tissue fragments. The standard bath solution was a high NaCl Ringer solution. The pipette solution was low Cl^- with aspartate being the principal anion and Na^+ the principal cation plus 5mM ATP and 5mM BAPTA. K^+ was omitted from all solutions. Reversal potentials were determined by polynomial regression of current-voltage records and inward conductance was measured between Vm = -120 to -100 mV. Data are expressed as means ± SEM and statistical significance was tested using Student's t test and assumed at the 5% level.

Mouse choroid plexus epithelial cells exhibited an inwardly rectifying conductance of 128 ± 24 pS/pF (n=20). The reversal potential was -2.6±1.3mV, suggesting a non-selective conductance. To investigate the identity of the inwardly rectifying conductance in more detail the effect of substituting bath Na^+ for other monovalent cations was examined. Replacing bath Na^+ with Cs^+ increased inwardly rectifying conductance to 596±74 pS/pF (n=5) whereas Li^+ and $NMDG^+$ caused the conductance to decrease to 30±6 and 17±3 pS/pF, respectively (n=9/5). The corresponding cation selectivity sequence of the inwardly rectifying conductance was equally selective for Cs^+ and Na^+ and much less selective for Li^+ and $NMDG^+$. Addition of 100μM gadolinium inhibited the conductance by 81±2% with no effect on outward current.

These data show that the epithelial cells of the choroid plexus express a non-selective cation conductance which is inhibited by gadolinium. The properties of the conductance described here are similar to those of some TRP channels, notably TRPM3, mRNA for which has recently been identified in murine choroid plexus tissue (Oberwikler et al. 2005).

Nilius B & Voets T (2005). Pflügers Arch 451, 1-10.

Oberwinkler J et al. (2005). J Biol Chem 280, 22540-22548.

This work was supported by the Wellcome Trust.

Where applicable, the authors confirm that the experiments described here conform with the Physiological Society ethical requirements.

PC17

Intermediate conductance Ca^{2+}-activated K^+ channels ($K_{Ca}3.1$) are not involved in basal Na^+ transport in absorptive human airway epithelial cells (H441)

S.M. Wilson, N. McTavish, S.G. Brown, R.P. McNeill, M.T. Clunes and R.E. Olver

Maternal and Child Health Sciences, University of Dundee, Dundee, UK

Epithelial Na^+ absorption depends upon K^+ channel activity (Gordon & MacKnight, 1991) and Ba^{2+} thus inhibits Na^+ absorption in human airway epithelia. Whilst the target K^+ channel has not been identified, there is evidence for $K_{Ca}3.1$ involvement (Gao et al. 2001; Clunes et al. 2005; McNeill et al. 2005), and so we cloned this channel from H441 cells, expressed it in CHO cells and studied its properties by recording currents from single cells held under voltage clamp. When $[Ca^{2+}]_i$ was buffered (5 mM EGTA) at 0.5 μM, $K_{Ca}3.1$ expression was associated with large, clotrimazole-sensitive (10 μM) currents (Fig. 1A) that reversed at a potential close to E_K (Fig. 1B). Increasing $[K^+]_o$ (Na^+ replacement) depolarised these cells in the manner predicted for a selective K^+ conductance (Fig. 1C) and so, under these conditions, the electrical properties of transfected cells are dominated by a selective K^+ conductance. However, $K_{Ca}3.1$ expression had no overt effect upon membrane conductance when $[Ca^{2+}]_i$ was 0.2 μM, although EBIO (1 mM) increased conductance under these conditions but had no effect upon the currents recorded at 0.5 μM $[Ca^{2+}]_i$ (Fig. 1D). This is consistent with the view that EBIO sensitizes $K_{Ca}3.1$ to Ca^{2+} (Pedersen et al. 1999). $K_{Ca}3.1$ thus appears inactive when $[Ca^{2+}]_i$ is ~0.2 μM suggesting that this channel does not contribute to resting K^+ conductance (G_K). Indeed, patch clamp studies of H441 cells, undertaken in the presence of amiloride (10 μM, included to block G_{Na}), showed (n = 6) that 10 μM clotrimazole had no effect upon V_m in unstimulated cells (control: 47.5 ± 6.7 mV, clotrimazole: 48.0 ± 6.8 mV) despite a clear, K^+-evoked depolarization (control: 52.8 ± 6.8 mV, 113 mM K^+: 25.7 ± 4.0, $P < 0.001$, Student's paired t test).

$K_{Ca}3.1$ expression thus appears to confer a latent K^+ conductance upon the membrane that is activated by increased $[Ca^{2+}]_i$ or EBIO. However, since these channels do not contribute to resting G_K, they cannot be involved in basal Na^+ absorption.

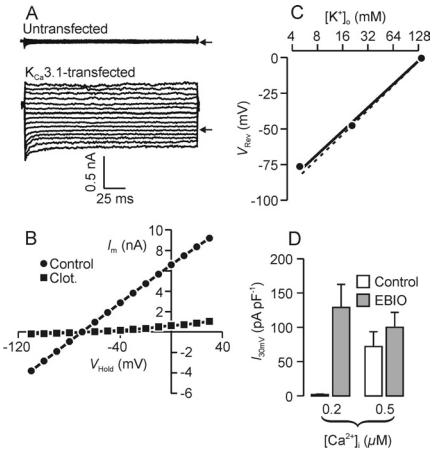

Figure 1. (A) Membrane currents recorded from control and $K_{Ca}3.1$-transfected CHO cells. (B) Current-voltage relationship for $K_{Ca}3.1$-expressing cells under control conditions and after clotrimazole (10 μM application. (C) relationship between V_{Rev} and $[K^+]_o$ for $K_{Ca}3.1$-expressing cells. The continuous line was fitted to the data by linear regression whilst the dashed line shows the relationship for a perfectly selective K^+ conductance (Nernst equation). (D) Membrane currents recorded at 30 mV from $K_{Ca}3.1$-expressing cells under control conditions and after application of EBIO (1 mM), data from experiments in which $[Ca^{2+}]_i$ was 0.2 μM and 0.5 μM.

Clunes MT, McNeill RP & Wilson SM (2005). J Physiol 565P, C122.

Gao L, Yankaskas JR, Fuller CM, Sorscher EJ, Matalon S, Forman HJ & Venglarik CJ (2001). Am J Physiol Lung Cell Mol Physiol 281, L1123-L1129.

Gordon LGM & MacKnight A (1991). J Memb Biol 120, 155-163.

McNeill RP, Clunes MT, Chambers LA & Wilson SM (2005). J Physiol 565P, C10.

Pedersen KA, Shrøder RL, Skaaning-Jensen B, Strøbæk D, Olesen S-R & Chrosophersen P (1999). Biochim Biophys Acta 1420, 231-240.

The authors are grateful to the Wellcome Trust and to Tenovus Scotland for their financial support.

Where applicable, the authors confirm that the experiments described here conform with the Physiological Society ethical requirements.

PC18

The functional role of tyrosine56 in the rabbit proton-peptide cotransporter, PepT1 expressed in *Xenopus* oocytes

M. Pieri[1], C.A.R. Boyd[1], P. Bailey[2] and D. Meredith[1]

[1]Physiology, Anatomy & Genetics, University of Oxford, Oxford, UK and [2]School of Chemistry, University of Manchester, Manchester, UK

PepT1 mediates the intestinal absorption and renal re-absorption of di- and tri-peptides and a great number of therapeutically active compounds (Daniel & Kottra, 2004). It has previously been proposed that a conserved histidine (H57) in the second transmembrane domain (TMD2) of the transporter is

protonated and binds the carboxy terminus of the substrate (Bailey *et al.* 2000). Tyrosine56 (Y56) is the adjacent residue to this histidine and has been proposed to stabilize the positive charge on the protonated histidine (Chen *et al.* 2000). Here we report the findings of further testing the role of Y56 by site-directed mutagenesis.

Tyrosine56 was mutated to a phenylalanine (giving Y56F-PepT1), and expressed in *Xenopus* oocytes. Both membrane expression and the transport properties of Y56F-PepT1 were determined by luminometry and uptake of 0.4μM [^{3}H]-D-Phe-L-Gln respectively using techniques previously described (Panitsas *et al.* 2006). Data are means ± SEM of n oocyte preparations.

As can be seen in Fig. 1, the uptake of D-Phe-L-Gln into oocytes expressing Y56F-PepT1 was significantly slower than for those expressing wild-type PepT1 (wt-PepT1), even when the level of protein surface expression is taken into account. Comparing the affinity for Gly-L-Gln revealed that the mutant had a greatly increased affinity for this neutral dipeptide, with a Ki at pHout 5.5 of 6 ± 1μM for Y56F-PepT1 compared with 324 ± 82μM for wt-PepT1 (n=4). This higher affinity was maintained at pHout 7.4 (5 ± 1μM and 244 ± 33μM for Y56F-PepT1 and wt-PepT1, respectively, n=3).

The finding that the affinity of Y56F-PepT1 is so dramatically different from that of wt-PepT1 suggests that Y56 either directly forms part of, or exerts an influence on, the substrate binding site of PepT1. One possible explanation is that Y56 stabilises H57 residue when in its deprotonated (rather than protonated) form, and thus when this effect is removed the substrate binds more tightly. This is consistent with the reduction in the rate of transport seen with Y56F-PepT1, with the release of the substrate from the binding site after translocation becoming the slowest step in the transport cycle.

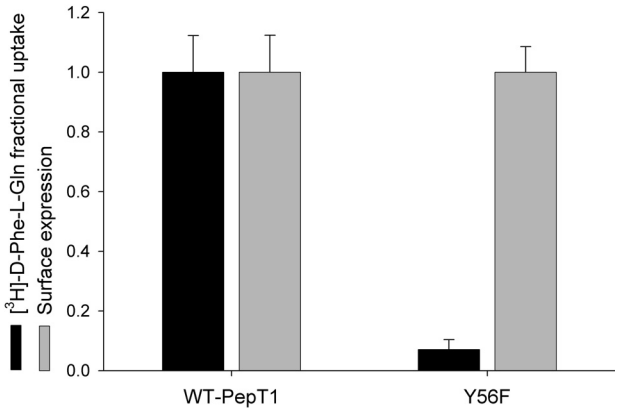

Figure 1. Normalised uptake of D-Phe-L-Gln and transporter surface expression in *Xenopus* oocytes expressing wild-type PepT1 (wt-PepT1) or Y56F-PepT1. The Y56F-PepT1 uptake is reduced to <10% of that of the wild-type ($p<0.01$, Student's paired t test, n=3).

Daniel H & Kottra G (2004). *Pflugers Arch* **447**, 610-618.

Bailey PD *et al.* (2000). *Angew Chemie Int Ed* **39**, 505-508.

Chen XZ *et al.* (2000). *Biochem Biophys Res Comm* **272**, 726-730.

Panitsas KE *et al.* (2006). *Pflugers Arch* (in press).

We thank the Wellcome Trust for their generous support.

Where applicable, the authors confirm that the experiments described here conform with the Physiological Society ethical requirements.

PC19

Passive permeability of the mouse placenta to mannitol is reduced in parathyroid hormone related protein (PTHrP) null conceptuses

H. Bond[1], B. Baker[1], R. Boyd[1], E. Cowley[1], J. Glazier[1], C. Sibley[1], B. Ward[1] and S. Husain[2]

[1]Division of Human Development, The University of Manchester, Manchester, UK and [2]Queen Mary College, University of London, London, UK

PTHrP plays an important role in fetal growth and skeletal development, regulating trophoblast and placental differentiation and placental calcium transport (Clemens *et al.* 2001). We have previously shown that the unidirectional maternofetal clearance of calcium is raised across the placenta of the PTHrP$^{-/-}$ (NL) fetuses when compared with their PTHrP$^{+/+}$ (WT) and PTHrP$^{+/-}$ (HZ) counterparts, suggesting placental transport function is altered (Bond *et al.* 2004). Here we test the hypothesis that there is altered passive permeability across the NL placenta. Using a technique recently devised for artificially perfusing the fetal circulation of the mouse placenta (Bond *et al.* 2006) we measured unidirectional maternofetal clearance of ^{14}C-mannitol (^{mannitol}Kmf), an inert hydrophilic tracer, across NL, WT and HZ placentas.

Heterozygote mice were mated and on day 18 of gestation (term=19-20d) were anaesthetised (i.p. fentanyl citrate/fluanisone: 24 and 750μg) and the uterus delivered into a saline bath at 40°C. A fetus was randomly selected, the umbilical artery and vein catheterised and perfused with Krebs Ringer (pH 7.4) at 60 μl/min. ^{14}C-mannitol (5μCi/50 μl saline) was injected via a maternal tail vein. Perfusate samples were collected every 5 min for 45 min. ^{mannitol}Kmf was calculated as: perfusate [^{14}C-mannitol] x perfusion rate/maternal plasma [^{14}C-mannitol] x placental weight. Data for ^{mannitol}Kmf are calculated as mean value over 45 min perfusion. Results are given in Table 1, expressed as mean±SEM. Statistical analysis used was one-way ANOVA followed by Tukey's post hoc test.

^{mannitol}Kmf was significantly reduced across the placenta(***$P<0.001$), whilst placental weight and P:F weight ratio were increased (*$P<0.05$; ***$P<0.001$ respectively), in the NL relative to WT and HZ. There was no significant reduction in NL fetal weight. These data suggest that in conceptuses lacking PTHrP the passive permeability of the placenta is reduced. This provides evidence that PTHrP may have an important role in determining placental exchange barrier properties as well as trophoblast growth.

Table 1

Genotype	WT	HZ	NL
^{mannitol}Kmf (μl/min/g placenta)	15.3±0.5 (n=3)	18.4±0.9 (n=8)	11.2±0. 2*** (n=5)
Placental weight (P) (g)	0.085±0.002 (n=30)	0.089±0.002 (n=64)	0.095±0.003* (n=24)
Fetal weight (F) (g)	0.87±0.01 (n=28)	0.85±0.01 (n=62)	0.83±0.02 (n=17)
P:F %	10.1±0.2 (n=27)	10.2±0.2 (n=58)	11.8±0.5*** (n=17)

Clemens *et al.* (2001). *Br J Pharmacol* **124**, 1113-1136.

Bond *et al.* (2004). *J Physiol* **565P**, C157.

Bond *et al.* (2006). *Trophoblast Research* (in press).

Supported by the Wellcome Trust.

Where applicable, the authors confirm that the experiments described here conform with the Physiological Society ethical requirements.

PC20

Properties of Ba^{2+} block of an inwardly rectifying K^+ conductance in cultured mouse collecting duct cells

H.C. Taylor[1], A. Ong[2] and L. Robson[1]

[1]Biomedical Science, University of Sheffield, Sheffield, UK and [2]Academic Nephrology Unit, Sheffield Kidney Institute, Division of Clinical Sciences (North), University of Sheffield, Sheffield, UK

The renal collecting duct is composed of principal and intercalated cells, which serve to control the extracellular fluid volume and solute composition of the body. Inwardly rectifying K^+ channels play an important role in collecting duct function. The aim of the following study was to examine an inwardly rectifying K^+ conductance in a cultured mouse collecting duct cell line (M8). K^+ currents were examined using the whole cell patch clamp technique. Clamp potential was stepped from a holding value of –40 mV, to between +100 and -100 mV in 20 mV steps. The current sensitive to 5 mM Ba^{2+} was measured in the presence of 135 mM KCl or 130 mM NaCl plus 5 mM KCl in the bath (both at pH 7.4 with 2 mM $CaCl_2$). The pipette solution contained 145 mM KCl with no added Ca^{2+} plus 0.5 mM EGTA (pH 7.4). Measurements were taken initially (~50 mS) after changing the potential and at steady state (SS) (~350 mS). Point conductance was calculated at +100 (G_{out}) and –100 mV (G_{in}). All values are expressed as means ± SEM. Statistical significance was tested using Student's unpaired t test and assumed at the 5% level.

With high KCl in the bathing solution the initial Ba^{2+}-sensitive G_{out} was 86.58 ± 32.37 μS/cm^2 and the initial G_{in} was 159.22 ± 49.92 μS/cm^2 (n=8). G_{in} was significantly greater than G_{out} identifying a weak inwardly rectifying K^+ conductance. SS conductances were not significantly different to initial values. With high NaCl in the bathing Ringer solution the initial Ba^{2+}-sensitive G_{out} was 140.60 ± 19.81 μS/cm^2 (n=48). At 350 ms Ba^{2+}-sensitive G_{out} had fallen to –9.69 ± 4.50 μS/cm^2. The initial Ba^{2+}-sensitive G_{in} was 53.51 ± 5.45 μS/cm^2 (n=48) and this increased at 350 ms to 64.73 ± 7.76 μS/cm^2. Time-dependent changes in G_{out} and G_{in} were not observed with total whole cell conductances.

These data are consistent with time-dependent changes in Ba^{2+} sensitivity of the whole cell K^+ conductance in the presence of extracellular Na^+. One explanation is that is at positive potentials Ba^{2+} ions are repelled out of the channel pore. The absence of time-dependent changes in Ba^{2+} sensitivity in the presence of extracellular K^+ could reflect the presence of a K^+ lock-in site, which prevents Ba^{2+} from leaving the pore when K^+ is bound (Spassova & Lu 1999; Vergara *et al.* 1999).

Spassova M & Lu Z (1999). J Gen Physiol 114, 415-426.

Vergara C, Alvarez O & Latorra R (1999). J Gen Physiol 114, 365-376.

This work was supported by the MRC.

Where applicable, the authors confirm that the experiments described here conform with the Physiological Society ethical requirements.

PC21

Basolateral K^+ conductance is decreased during cAMP-stimulated Cl^- secretion in human colonic crypts

J.E. Linley[1,2], A.A. Al-Hazza[1], A. Loganathan[1], G.I. Sandle[2] and M. Hunter[1]

[1]Institute of Membrane and Systems Biology, University of Leeds, Leeds, UK and [2]Institute of Molecular Medicine, University of Leeds, Leeds, UK

The current model of Cl^- secretion in mammalian colonic crypts involves electroneutral Cl^- entry across the basolateral membrane, facilitated by Na^+-K^+-2Cl^- co-transport, followed by electrogenic Cl^- exit across the apical membrane through cAMP activated Cl^- channels. Simultaneous activation of basolateral K^+ channels is thought to maintain a favourable electrical gradient for apical Cl^- secretion by limiting cell depolarisation. In this study we have sought evidence for K^+ channel activation by cAMP using perforated whole cell patch clamp in human colonic crypts.

Sigmoid biopsies were obtained from patients undergoing routine colonoscopy for altered bowel habit. Colonic crypts were isolated using a Ca^{2+} chelation technique as described previously (Bowley *et al.*, 2003). Slow-whole cell currents (with amphotericin B in the pipette) were measured from colonocytes in the mid-third of intact crypts. Single channel currents were measured from the basolateral membrane using the cell attached patch technique. Data are presented as mean ± 1 SEM, with n, the number of experiments. Comparison was by paired t test with significance assumed at $p < 0.05$.

Under basal conditions, whole cell currents were predominantly K^+ selective with a conductance (G) of 0.98 ± 0.1 nS and a reversal potential (E_{rev}) of -62 ± 2 mV (n = 40). Forskolin (FSK, 10 μM) gave a ~3 fold increase in G and a depolarising shift in E_{rev} of 29.8 ± 7 mV (n = 8, $P < 0.05$). The FSK-stimulated conductance was significantly inhibited by removal of bath Cl^- (107 ± 3%, n = 8), or addition of NPPB (200 μM; 85 ± 18%, n = 4) but not DIDS (100 μM; 1 ± 8%, n = 4), indicating activation of CFTR. The effect of FSK on GK^+ was investigated under low Cl^- conditions (4mM Cl^- in bath and pipette), where FSK reduced the basal conductance from 1.43 ± 0.6 nS to 0.56 ± 0.1 nS (n = 6, $P < 0.05$) and depolarised the cell from -62 ± 4 to -44 ± 8 mV ($P < 0.05$), consistent with K^+ channel inhibition. Addition of chromanol 293B (10 μM), an inhibitor of the cAMP-activated K^+ channel KCNQ1, to FSK-stimulated crypts, was without effect in both high and low Cl^- experiments. Single channel analysis of the basolateral membrane revealed that intermediate conductance Ca^{2+}-sensitive K^+ channels (IK_{Ca}) were inhibited by forskolin (n = 7, $p<0.05$).

In conclusion, FSK stimulated a Cl^- conductance with pharmacological properties consistent with CFTR. We found no evidence of K^+ channel activation by cAMP in human colonic crypts. Paradoxically, FSK inhibited the basal whole cell K^+ conductance and basolateral IK_{Ca} channels suggesting that basolateral K^+ channels have a permissive, yet limiting, role in Cl^- secretion in human colonic crypts.

Bowley KA, Morton MJ, Hunter M & Sandle GI (2003). *Gut* **52**, 854-860.

Supported by Yorkshire Cancer Research.

Where applicable, the authors confirm that the experiments described here conform with the Physiological Society ethical requirements.

PC22

Expression and sub-cellular distribution of the two-pore channel 1 (tpc1) in mouse renal collecting duct cells

S.A. John[1], G. Carr[1], E.L. Morgan[2], G.L. Kellett[2] and N.L. Simmons[1]

[1]Cell and Molecular Biosciences, University of Newcastle upon Tyne, Newcastle upon Tyne, UK and [2]Biology, University of York, York, UK

The gene encoding the mammalian two-pore channel 1 (tpc1) is homologous to the *Arabidopsis thaliana,* tpc gene, which encodes a class of Ca^{2+}-dependent Ca^{2+}-release channels present in the vacuolar membrane (Maathuis et al. 2005). tpc1 is expressed in epithelial tissues including the kidney where it is expressed in the collecting duct (Ishibashi et al. 2000). In order to investigate the possible physiological functions of tpc1 in renal collecting duct cells we have determined the expression and sub-cellular location of tpc1 in mouse renal collecting duct cell-lines (M1, mIMCD-K2 and mIMCD-3).

Using gene-specific primers for murine tpc1 we have detected expression of tpc1 in all 3 cell-lines by RT-PCR of a 450bp PCR product confirmed by direct sequencing. Using IMAGE clone 6821376 as template, tpc1 was cloned into expression vector pcDNA3.1/NT-GFP producing a tpc1/N-terminal GFP construct (tpc1-NT-GFP). Sub-cellular localisation of tpc1-NT-GFP was determined after Lipofectamine-mediated transfection of sub-confluent mIMCD-3 cells grown on coverslips. Cells were imaged 24-48 h post-transfection, using confocal microscopy as previously described (Sayer et al. 2001). Alternatively a TPC1 antibody raised against a C-terminal peptide AAQQTPGSRQRSQTVT was used to localise mtpc1 by immunohistochemistry on filter grown collecting duct cell-lines.

In mIMCD-3 cells tpc1-NT-GFP localised to the plasma membrane and intracellular vesicles. Plasma membrane expression was confirmed by brief (2 min) incubation with TRITC conjugated wheat germ lectin prior to methanol fixation and imaging. The nature of the vesicular compartment was further investigated in mIMCD-3 cells by counter staining with Lysotracker Red (marker of acidic endosomes) and by cotransfection with an mCLC-5-CT-RFP fusion (marker of recycling early endosomes) or pDsRED-ER (endoplasmic reticulum marker). Whereas there was minimal overlap with Lysotracker Red or mCLC-5-CT-RFP, there was substantial co-localisation of tpc1-NT-GFP with the endoplasmic reticulum marker.

In all 3 cell-lines immunohistochemistry revealed prominent sub-apical vesicular staining.

We conclude that the location of tpc1 is consistent with its possible role as a Ca^{2+}-influx pathway and as a Ca^{2+}-release channel for Ca^{2+} stores in epithelial tissue including the mammalian collecting duct.

Ishibashi K, Suzuki M & Imai M (2000). Biochem Biophys Res Comm 270, 370-376.

Maathuis PE, Mills FJ, Knight H, Pelloux J, Hetherington AM & Sanders D (2005). Nature 434, 404-408.

Sayer JA, Stewart GS, Boese SH, Gray MA, Pearce SHS, Goodship THJ & Simmons NL (2001). J Physiol 536, 769-783.

Supported by Kidney Research UK.

Where applicable, the authors confirm that the experiments described here conform with the Physiological Society ethical requirements.

PC23

Differential regulation of the apical plasma membrane calcium pump by protein kinase-A in mouse parotid acinar cells

J.I. Bruce[1], S. McLarnon[1], D. Topham[1], H. Isom[1], D.I. Yule[2] and T.J. Shuttleworth[2]

[1]Faculty of Life Sciences, University of Manchester, Manchester, UK and [2]Department of Pharmacology and Physiology, University of Rochester Medical Centre, Rochester, NY, USA

Effective fluid secretion in parotid acinar cells is dependent on the spatio-temporal regulation of intracellular Ca^{2+} ($[Ca^{2+}]_i$) signals by cAMP. Such signalling cross-talk allows exquisite control of spatially distinct ion fluxes which maintain maximum water movement. Previous studies have demonstrated that the key molecular mechanisms for this signalling cross-talk is the PKA-mediated modulation of Ca^{2+} release and Ca^{2+} clearance [1,2]. The plasma membrane Ca^{2+}-ATPase (PMCA), an important Ca^{2+} clearance pathway, maintains low resting $[Ca^{2+}]_i$ and is also dynamically regulated by Ca^{2+} in an integrative manner, important for modulating $[Ca^{2+}]_i$ oscillations. In addition, the PMCA binds to multi-protein signalling complexes, important for regulating local $[Ca^{2+}]_i$ signals and thus local Ca^{2+}-dependent effectors. Previous studies have demonstrated in parotid acinar cells that PKA potentiates and phosphorylates the PMCA but only in the presence of $[Ca^{2+}]_i$-raising agents (2). Therefore, the aim of the present study was to determine, (i) the expression and spatial distribution of specific PMCA isoforms; (ii) which of these PMCA isoforms are regulated by PKA in a Ca^{2+}-dependent manner and, (iii) how this differentially regulates the spatial $[Ca^{2+}]_i$ clearance in parotid acinar cells.

Fura-2-loaded parotid acinar cells were treated with 30 μM cyclopiazonic acid to inhibit the ER Ca^{2+}-ATPase (SERCA) and raise $[Ca^{2+}]_i$. Clearance of $[Ca^{2+}]_i$ was initiated by removal of external Ca^{2+} and normalised by fitting to an exponential decay to obtain a time constant (τ). Activation of PKA (using 10 μM forskolin) differentially potentiated $[Ca^{2+}]_i$ clearance in the apical region (τ=32.2 ± 1.3), compared to the basal region (τ=56.2 ± 1.0; n=5, $p<0.05$ using a non-parametric Mann-Whitney test), whereas in control cells apical and basal $[Ca^{2+}]_i$ clearance was not significantly different (apical τ=49.2 ± 2.8, basal τ=48.4 ± 2.0; n=4). Western blotting revealed that PMCA1, 2 and 4 are expressed in parotid acinar cells (n≥4). Immunofluorescence revealed that PMCA1 (n=3) was distributed throughout all regions of the plasma membrane, whereas PMCA4 (n=3) was localized to the apical membrane of parotid acinar cells. Likewise, the PDZ-containing accessory proteins, ezrin and EBP50 also exhibited an apical distribution. In situ phosphorylation assays demonstrated that PMCA1 (n=3) and PMCA2 (n=3)

were phosphorylated by the combined treatment with forskolin and CCh.

Collectively these data suggest that PMCA1 (or PMCA2) is phosphorylated by PKA in a Ca^{2+}-dependent manner that differentially regulates Ca^{2+} clearance in the apical region of parotid acinar cells. This probably involves a Ca^{2+}-mediated assembly of a signalling complex that brings PKA closer to the PMCA allowing targeted regulation specifically at the apical plasma membrane. Such tight spatial regulation of Ca^{2+} efflux may represent an important mechanism for the fine-tuning of Ca^{2+}-dependent effectors at the apical membrane important for the regulation of fluid secretion and exocytosis.

Bruce JIE *et al.* (2002a). *J Biol Chem* **277** (2), 1340-1348.

Bruce JIE *et al.* (2002b). *J Biol Chem* **277**(50), 48172-48181.

Where applicable, the authors confirm that the experiments described here conform with the Physiological Society ethical requirements.

PC24

Role of human concentrative nucleoside transporter 3 (hCNT3-SLC28a3) in determining vectorial flux of nucleosides and nucleoside-derived drugs across epithelia

E. Errasti, F. Casado and M. Pastor

Department of Biochemistry and Molecular Biology, University of Barcelona, Barcelona, Spain

The mechanisms implicated in the vectorial flux of nucleosides across polarized epithelia have not yet been characterized appropriately, neither is it known how hCNT3, a nucleoside transporter expressed in several segments of the nephron [1], contributes to this process. To address this issue, we have first used and characterized a cell line derived from murine proximal convoluted tubule (PCT), which expresses CNT3 as the only murine ortolog of the SLC28 gene family. PCT cells, when grown on transwell filters, show CNT3-type transport activity at the apical side. In the presence of sodium, H3-cytidine apical to basal flux is quantitatively relevant (240 ± 12 pmol/mg prot min) and associates with considerable nucleoside metabolism, thus resulting in uracil and uridine as major metabolites detected at the basal compartment. In the absence of sodium (CNT3 being inactive) a significant reduction in vectorial flux was found (60 ± 2 pmol/mg prot min, P>0.001 vs sodium), although most of the tracer at the basal side turned out to be the intact substrate, H3-cytidine. These data were mimicked in another cell model, MDCK cells, transiently transfected with the human ortolog of CNT3 (hCNT3). When using a GFP-tagged hCNT3 expression, and its corresponding functional activity, was found to be exclusively located at the apical side of the monolayer [2], in accordance with what we have also found for the endogenously expressed CNT3 of murine PCT cells. Apical insertion of hCNT3 results in a vectorial flux and nucleoside metabolism similar to that found in PCT cells in the presence of sodium, whereas data in the absence of the cation resembled those found in MDCK cells transfected with the empty vector. This cell model was further used to determine how hCNT3 insertion contributed to the vectorial flux of a panel of antiviral and antineoplasic nucleoside-derived drugs. Our data demonstrate that apical insertion of hCNT3 and, therefore, hCNT3 function itself, are major determinants of nucleoside and nucleoside-derived vectorial flux across epithelia.

Rodriguez-Mulero S et al. (2005). Kidney Int 68, 665-672.

Mangravite LM et al. (2003). Eur J Pharmacol 479, 269-281.

Where applicable, the authors confirm that the experiments described here conform with the Physiological Society ethical requirements.

PC25

The revertant mutants G550E and 4RK potentiate the gating behaviour of wild-type, ΔF508- and V562I-CFTR Cl^- channels

Z. Xu[1], M. Roxo-Rosa[2,3], Z. Cai[1], A. Schmidt[2], M. Neto[2], M.D. Amaral[2,3] and D.N. Sheppard[1]

[1]Physiology, University of Bristol, Bristol, UK, [2]Chemistry and Biochemistry, University of Lisboa, Lisboa, Portugal and [3]Centre of Human Genetics, National Institute of Health, Lisboa, Portugal

Removal of arginine-framed trafficking motifs (AFTs) allows misfolded membrane proteins to escape the endoplasmic reticulum (ER) quality control, rescuing their cell surface expression [1,2]. The simultaneous replacement of arginine by lysine at positions 29, 516, 555 and 766 (4RK) restored the processing and function of the cystic fibrosis transmembrane conductance regulator (CFTR) protein bearing ΔF508, the most common CF mutation [2]. Another ΔF508 revertant mutation (G550E), located within the conserved LSGGQ motif of nucleotide-binding domain 1 (NBD1) produced, by itself, a similar effect [1]. However, it is unknown whether G550E and 4RK rescue other CF mutants or affect the function of wild-type (WT)-CFTR. Here, we tested the effects of these revertants on WT-, ΔF508- and V562I-CFTR using excised inside-out membrane patches from BHK cells expressing each CFTR variant. The pipette (extracellular) solution contained 10 mM Cl^-, and the bath (intracellular) solution contained 147 mM Cl^-, ATP (1 mM) and PKA (75 nM) at 37°C; voltage was –50 mV. Data are means ± S.E.M. of n observations and statistical analyses were performed using Student's paired t test.

Temperature-rescued ΔF508-CFTR had a reduced open probability (P_o) with dramatically prolonged closures between bursts of openings. In contrast, V562I generated a regulated Cl^- channel with P_o, mean burst duration (MBD) and interburst interval (IBI) similar to WT (WT, $P_o = 0.47\pm0.04$, n = 6; ΔF508, $P_o = 0.06\pm0.01$, n = 10, $p < 0.001$; V562I, $P_o = 0.45\pm0.01$, n = 5, $p > 0.05$). 4RK only slightly increased the P_o of WT by doubling MBD and slightly prolonging IBI (4RK, $P_o = 0.54\pm0.04$, n = 2). However, G550E almost doubled the P_o of WT by increasing the MBD 4-fold, without affecting IBI (G550E, $P_o = 0.77\pm0.02$, n = 3, $p < 0.001$). 4RK in cis with ΔF508 increased P_o, but it was still lower than WT (ΔF508-4RK, $P_o = 0.23\pm0.02$, n = 13, $p < 0.001$); MBD was enhanced 5-fold, but IBI was unchanged. ΔF508-G550E had a much higher P_o than ΔF508 because MBD was increased 8-fold and IBI decreased 2.5-fold. For V562I, 4RK caused a slight increase in P_o (V562I-4RK, $P_o = 0.55\pm0.07$; n = 4; $p > 0.05$), but G550E greatly enhanced it (V562I-G550E, $P_o = 0.80\pm0.03$; n = 8; $p < 0.001$). Neither 4RK nor G550E altered the IBI of V562I.

However, 4RK prolonged MBD of V562I 2-fold and G550E 4-fold. Our data suggest that G550E enhances more strongly than 4RK the gating behaviour of WT, ΔF508 and V462I. They also suggest that V562I might not be a CF-causing mutation. Consistent with this idea, two individuals with the genotype ΔF508/V562I have no clinical signs of CF (P. Pacheco and C. Barreto, personal communications).

Zerangue N et al. (1999). Neuron 22, 537–548.

Chang X-B et al. (1999). Molecular Cell 4, 137-142.

DeCarvalho AC et al. (2002). J Biol Chem 277, 35896-35905.

Supported by research grants POCTI/1999/MGI/35737, POCTI/MGI/47382/2002 (Portugal) and CF Trust grants (UK). M.R.R. was a recipient of a PhD fellowship (PRAXIS BD/19869/99) (Portugal).

Where applicable, the authors confirm that the experiments described here conform with the Physiological Society ethical requirements.

PC26

Retinoic acid-induced changes in amino acid transport in human SH-SY5Y neuroblastoma cells

S.A. Harrison, T.R. Cheek and D.T. Thwaites

Institute for Cell & Molecular Biosciences, University of Newcastle upon Tyne, Newcastle upon Tyne, UK

The capacity of neuroblastoma cells to undergo differentiation in response to retinoids (Brown *et al.* 2005) is being targeted as the basis for development of novel retinoid-based therapeutic regimes for the treatment of neuroblastoma disease (Riddoch *et al.* 2005). Relatively little is known about the changes in expression of membrane transport proteins in neuroblastoma cells following differentiation but mapping these changes will be central to the development of novel treatments and therapies. Radiolabelled amino acid uptake (0.5μCi ml^{-1}, 0.1-500μM, 10min, 37°C) measurements were performed in a HEPES/Tris-buffered bicarbonate-free Krebs solution (pH 7.4) using human SH-SY5Y neuroblastoma cells grown on plastic in the presence or absence of 1μM 9 *cis*-retinoic acid (9*c*RA) for 7 days. 9*c*RA-induced differentiation had varying effects on uptake of a number of amino acids. Differentiation led to a decrease in [^{3}H]taurine [from 1243 ± 74 (54) to 405 ± 37 (54) pmol mg^{-1} $(10min)^{-1}$, $p<0.001$ unpaired two-tailed Student's *t* test], [^{3}H]proline [1046 ± 68 (21) to 558 ± 45 (21) pmol mg^{-1} $(10min)^{-1}$, $p<0.001$] and [^{3}H]glutamic acid [627 ± 58 (6) to 454 ± 35 (6) pmol mg^{-1} $(10min)^{-1}$, $p<0.05$] uptake, an increase in [^{3}H]lysine [1906 ± 131 (10) to 3756 ± 511 (10) pmol mg^{-1} $(10min)^{-1}$, $p<0.01$] uptake but no effect on uptake of [^{3}H]GABA [374 ± 27 (5) and 324 ± 48 (6) pmol mg^{-1} $(10min)^{-1}$, $p>0.05$]. All data are mean ± SEM (n). In undifferentiated cells, taurine uptake has many characteristics of the TauT transporter (Ramamoorthy *et al.* 1994) being a high affinity (K_m 26.6 ± 3.4 μM, r^2 = 0.954) Na^+ and Cl^--dependent carrier that is inhibited by unlabelled (all 1mM) taurine, β-alanine, GABA and β-ABA but not by proline, MeAIB, α-ABA, glycine, serine and valine. Taurine uptake had similar characteristics in differentiated cells but uptake was always significantly lower ($p<0.001$) than in undifferentiated cells. In conclusion, 9*c*RA-induced differentiation of SH-SY5Y neuroblastoma cells is associated with a change in expression of the complement of amino acid transporters expressed at the plasma membrane. Differentiation of SH-SY5Y cells is also associated with altered Ca^{2+} signalling (Brown *et al.* 2005; Riddoch *et al.* 2005). The nature of the relationship between altered cell signalling and transporter function requires further investigation.

Brown AM *et al.* (2005). *Biochem J* **388**, 941-948.

Ramamoorthy S *et al.* (1994). *Biochem J* **300**, 893-900.

Riddoch FC *et al.* (2005). *Cell Calcium* **38**, 111-120.

Supported by the MRC and BBSRC. S.A.H. holds an MRC postgraduate studentship.

Where applicable, the authors confirm that the experiments described here conform with the Physiological Society ethical requirements.

PC27

Apical Na^+-H^+ exchange in interlobular pancreatic ducts isolated from cystic fibrosis mice

A. Yamamoto[1], H. Ishiguro[1], S.B. Ko[2], T. Kondo[1], M. Lee[3] and S. Naruse[2]

[1]Human Nutrition, Nagoya University Graduate School of Medicine, Nagoya, Japan, [2]Gastroenterology, Nagoya University Graduate School of Medicine, Nagoya, Japan and [3]Pharmacology, Yonsei University College of Medicine, Seoul, South Korea

Na^+-H^+ exchangers (NHE) are localized in both basolateral and apical membranes of various epithelia and 8 isoforms have been identified. NHE3 is localized in the apical membrane and mediates HCO_3^- absorption in kidney proximal tubule and H^+-coupled dipeptide absorption in the small intestine. NHE activity was detected at the apical membrane of the main pancreatic duct from mice (1). In the present study, to investigate the role of apical NHE in HCO_3^- secretion from pancreatic duct cells, we examined the activity of apical NHE in interlobular pancreatic duct segments isolated from normal and ΔF mice, a cystic fibrosis mouse model in which the ΔF508 mutation was introduced in the mouse CFTR (cystic fibrosis transmembrane conductance regulator) and pancreatic HCO_3^- secretion is impaired.

Interlobular duct segments (~100 μm in diameter) were isolated by collagenase digestion and microdissection as described previously (2). The lumen was microperfused and intracellular pH (pH_i) was measured by microfluorometry at 37oC in ducts loaded with the pH-sensitive fluoroprobe BCECF (3). Both the bath and lumen were perfused with HCO_3^--free Hepes-buffered solutions. The duct cells were acid-loaded with a 2-min pulse of 20 mM NH_4^+, which was followed by a Na^+-free solution in both the bath and lumen. The rate of pH_i recovery after re-addition of Na^+ to the luminal solution was calculated as a measure of the activity of apical Na^+-H^+ exchange. Averaged data are presented as the mean ± SD. Tests for significant differences were made with Student's t test.

The rate of pH_i recovery (dpH/dt) (dependent on luminal Na^+, independent of HCO_3^-) was 0.12 ± 0.01 pH unit/min (n = 8) in wild type (WT/WT) ducts, which was completely inhibited by 100 μM HOE642, an inhibitor of NHE to 0.005 ± 0.003 pH

unit/min (n = 6, p < 0.01). Forskolin (1 μM), an activator of adenylate cyclase, reduced the apical NHE activity to 0.05 ± 0.01 pH unit/min (n = 9, p < 0.01). The apical NHE activity in cystic fibrosis (ΔF/ΔF) ducts was 0.20 ± 0.01 pH unit/min (n = 6), which was significantly (p < 0.01) higher than that in wild type ducts and was accelerated to 0.66 ± 0.11 pH unit/min (n = 6, p < 0.01) by application of forskolin.

In interlobular duct cells from mice pancreas, the activity of apical NHE was suppressed by functional CFTR and it was stimulated by cAMP in the absence of functional CFTR. These data suggest that the inhibitory regulation of apical NHE by CFTR does not work in cystic fibrosis pancreatic duct, which may lead to acidification of pancreatic juice.

Ahn W et al. (2001). J Biol Chem 276, 17236-17243.

Ishiguro H et al. (1998). J Physiol 511, 407-422.

Ishiguro H et al. (2000). J Physiol 528, 305-315.

Supported by grants from the Ministry of Education, Science, and Technology, Japan.

Where applicable, the authors confirm that the experiments described here conform with the Physiological Society ethical requirements.

PC28

Human bestrophin 1 is expressed in the human pancreatic duct cell line, CFPAC-1

L. Marsey and J.P. Winpenny

School of Medicine, Health, Policy and Practice, University of East Anglia, Norwich, Norfolk, UK

Calcium-activated chloride channels (CaCC) are major targets for an alternative anion channel therapy in cystic fibrosis (CF). The molecular identity of CaCC has yet to be defined. The bestrophins are a novel candidate for the molecular origin of CaCC (Sun et al. 2001; Qu et al. 2004). In this study, we provide the first evidence for the existence of human bestrophin 1 (hBest 1) in CFPAC-1 cells.

Native CaCC were characterised in confluent monolayers of CFPAC-1 cells using a non-radioisotope, iodide efflux assay. Application of ionomycin to CFPAC-1 monolayers led to a concentration-dependent increase in iodide efflux. Maximal efflux was observed with 2 μM ionomycin, which induced an increase in efflux of 14.6 ± 1.9% (n = 4, p<0.001). Niflumic acid (200 μM) inhibited the response demonstrated with 0.5 μM ionomycin from 7.7 ± 1.3% to 1.8 ± 1.3% (n = 4, p<0.001). The purine receptor agonist, uridine 5'-triphosphate (UTP), also stimulated efflux from CFPAC-1 monolayers in a concentration dependent manner. Maximal efflux was observed at 200 μM UTP (9.0 ± 1.6%, n = 6, p<0.001). Niflumic acid (200 μM) reduced the response elicited by 100 μM UTP from 7.9 ± 2.0% to 1.99 ± 0.13% (n = 6, p<0.001) and 500 μM 4,4'-diisothiocyanatostilbene-2,2'-disulfonate (DIDS) also reduced the response from 7.9 ± 2.0% to 2.2 ± 1.5% (n = 6, p<0.001).

Total RNA was isolated from CFPAC-1 cells and RT-PCR was carried out with hBest1 specific primers corresponding to three areas of the cDNA sequence (NM 004183, Genbank database). RT-PCR yielded three bands of 489, 461 and 411 base pairs, respectively, identical in size to the predicted products. Sequence analysis of the three products demonstrated 100% sequence identity to that published in GenBank, indicating that the three products were consistent with the hBest1 gene. To assess the expression of hBest 1 at the cellular level, two commercially available antibodies were used, ab 14927 (Abcam, UK) and Bst 121 (Fabgennix, USA). Western blot analysis of CFPAC-1 protein isolates showed that both antibodies gave similar blots (n=8 and n=4, respectively), with a principal band at approximately 55 kDa and three very faint bands around 70, 75 and 78 kDa.

To further confirm the expression of hBest 1 in CFPAC-1 cells, the cells were fixed with 4% paraformaldehyde and hBest1 was labelled using either ab 14927 (n=3) or Bst 121 (n=2). Preliminary confocal image analysis of the fixed cells showed that hBest 1 is expressed to a large degree in the cytoplasm, most probably in cytoplasmic vesicles. Although not immediately obvious, some staining may be confined to the plasma membrane.

Taken together, these preliminary data suggest that hBest 1 is expressed in the CFPAC-1 cell line. Further studies are being undertaken to determine whether other bestrophin homologues are expressed in CFPAC-1 cells.

Sun H et al. (2001). Proc Nat Acad Sci 99(6), 4008-4013.

Qu Z et al. (2004). J Gen Physiol 123, 327-340.

Where applicable, the authors confirm that the experiments described here conform with the Physiological Society ethical requirements.

PC29

Fatty acid and particle sensing mechanisms in epithelial and endocrine cells

A.D. Jackson, A.J. Higgins, R.M. Case and J.T. McLaughlin

Tissues to Organisms, University of Manchester, Manchester, UK

The murine enteroendocrine cell line STC-1 responds to fatty acids (FA) by secreting biologically active CCK, via an elevation of intracellular calcium, $[Ca^{2+}]_i$. This therefore represents a tractable model of FA sensing. Previous work has suggested that the formation of aggregates by FA in physiological media is an important factor in lipid sensing by STC-1 cells (Kazmi et al. 2003). Synthetic latex microspheres (LM) of similar size to FA aggregates (~90-300nm) also stimulate STC-1 cells causing CCK secretion, raising the possibility that these are sensed by the same cellular mechanism as FA. The cellular mechanism(s) underlying FA sensing remain largely uncharacterized, although one candidate is the newly assigned FA receptor, GPR40, first described in pancreatic beta cells, but which is also expressed by STC-1 cells. We therefore evaluated (1) if LM activate GPR40, and (2) if other cell models sensitive to LM are also FA sensitive. Real-time changes in $[Ca^{2+}]_i$ were measured using fura-2-loaded cells challenged with FA (linoleic acid, C18:2) and LM, by measuring a rise in the fura-2 340/380 ratio value which corresponds to a rise in intracellular calcium. Initially, RT-PCR confirmed expression of GPR40 in STC-1 but not in (rat) neuroendocrine PC12 cells. mGPR40 was therefore subcloned from STC-1 cells and stably overexpressed in PC12 cells. PC12 sensitivity to FA was increased 2.5-fold in PC12 mGPR40+ cells versus wild type cells (P=0.005, Mann-Whitney *U* test); PC12 mGPR40+ cells

responded to 500μM C18:2 with a rise in the fura-2 340/380 ratio value of 0.4±0.05 (n=5) compared to 0.16±0.02 (n=5) in PC12 WT cells. As with STC-1 cells, PC12-WT cells also responded to LM with a 0.23±0.06 (n=6) rise in 340/380 ratio value, but LM sensitivity was not significantly altered in mGPR40+ PC12 cells. Furthermore, the $[Ca^{2+}]_i$ response to LM was entirely abolished in the absence of extracellular calcium, whilst the FA-induced $[Ca^{2+}]_i$ response was preserved. Finally, a $[Ca^{2+}]_i$ response was also induced by LM in both MDCK (canine renal tubule epithelial model) and CaCo-2 (human intestinal epithelial model) cell lines, but not induced by FA in either. In conclusion, cell stimulation by LM is not via GPR40, nor is it a property restricted to FA-sensitive epithelial cells. This indicates that LM are not mimicking FA aggregates by activating specific FA-sensing mechanism(s). The mechanisms by which LM gate intracellular calcium entry remain to be elucidated. Nonetheless, LM induce CCK secretion in enteroendocrine cells, so may provide a novel method by which to modify upper gastrointestinal function or satiety, employing a non-nutrient signal that is retained within the lumen of the GI tract.

Kazmi S et al. (2003). J Physiol 553, 759-773.

Supported by BBSRC and Bristol Myers Squibb.

Where applicable, the authors confirm that the experiments described here conform with the Physiological Society ethical requirements.

PC30

Fatty acid sensing by GPR40 heterologously expressed in PC12 cells

A.J. Higgins, A.D. Jackson, J.T. McLaughlin and C.P. Smith

Tissues to Organisms, University of Manchester, Manchester, UK

Fatty acid (FA) sensing mechanisms in gut epithelia remain undefined, but enteroendocrine cells (EEC) play a pivotal role. One potential candidate sensor is the recently deorphanised receptor GPR40, originally identified in pancreatic β cells (Itoh *et al.* 2003). The murine enteroendocrine cell line, STC-1, is known to express GPR40 and is responsive to FA in a chain length-dependent manner. This requires a minimum acyl chain length of 12 carbons, as is observed *in vivo* in humans. The aim of this study was therefore to express mouse GPR40 in a heterologous system, and study whether the chain length specificity of transferred fatty acid responsiveness is preserved. Initially, mGPR40, obtained by RT-PCR from the STC-1 cell line, was subcloned into the mammalian expression vector pEYFP-N1 in C-terminal fusion with the fluorescent protein EYFP, then stably expressed in the neuroendocrine cell line, PC12. Both wild type (WT) and mGPR40EYFP-expressing PC12 cells were loaded with Fura-2 to monitor $[Ca^{2+}]_i$ by fluorescence microscopy.

As observed in humans and STC-1 cells, FA of acyl chain length C4-C10 did not increase $[Ca^{2+}]_i$ in either PC12-WT or mGPR40EYFP+ cells. However, mGPR40EYFP+ PC12 cells displayed significantly increased $[Ca^{2+}]_i$ responsiveness to long chain FA compared to PC12-WT cells. Dodecanoic acid (C12:0) produced no increase in $[Ca^{2+}]_i$ in PC12-WT, but a large response was elicited in mGPR40EYFP+ PC12 cells, with an average ratio increase of 0.5±0.08 ratio units (n=5). Linoleic acid (C18:2) induced a small rise in $[Ca^{2+}]_i$ in PC12-WT (0.1±0.05 ratio units, n=3) which was amplified in mGPR40EYFP+ PC12 cells (0.4±0.05 ratio units, n=4; $P<0.05$, Mann-Whitney *U* test). For comparison, the maximal $[Ca^{2+}]_i$ response induced by 70mM KCl was 0.7±0.1 ratio units in PC12-WT and 0.6±0.1 ratio units in mGPR40EYFP+ PC12 cells. Responses were both reversible and reproducible. Data values are mean±SEM. In conclusion, mGPR40 heterologously expressed in the PC12 neuroendocrine cell line retains chain length-dependent FA responses entirely concordant with previous studies in both the STC-1 cell line and in humans, further supporting a functional role for GPR40 in gut FA-sensing by EEC. These data justify further detailed study into the signalling pathways and detailed molecular physiology of the GPR40 receptor in relation to EEC.

Itoh Y et al. (2003). Nature 422(6928), 173-176.

This research was funded by the BBSRC.

Where applicable, the authors confirm that the experiments described here conform with the Physiological Society ethical requirements.

PC31

Roles of the N- and C-termini in the function of the urea transporter mUT-A3

V.M. Collins and G.J. Cooper

Department of Biomedical Science, University of Sheffield, Sheffield, UK

Urea transporters play an integral role in the urinary concentration process. UT-A3 is expressed basolaterally in cells lining the inner medullary collecting duct (Stewart *et al.* 2004). Although much is known about the regulation and distribution of UT-A3, we have little idea how these proteins function at the molecular level. The current study evaluates the role of the N- and C-termini in the function of the mouse urea transporter UT-A3 (mUT-A3).

In all experiments mUT-A3 and its mutations have been N-terminally tagged with eGFP. Truncation and point mutations were constructed using standard PCR techniques. All mutations were confirmed by sequencing. Oocytes were isolated from Xenopus laevis and injected with 1.5ng of cRNA encoding mUT-A3, its mutants or 50nl of water. Urea transport was assessed 3-4 days after injection by measuring uptake of ^{14}C-labelled urea as described previously (Fenton *et al.* 2000). Statistical analysis was performed using one way ANOVA coupled with the Student-Newman-Keuls test. Results were obtained from at least 10 oocytes, isolated from 2 or more animals. Significance has been assumed at the 5% level.

The N-terminal of mUT-A3 was shortened, to start at residues M55 and M111. The M55-start mutant was functional when expressed in oocytes. M111-start, was non-functional suggesting a region between M55 and M111 is important for mUT-A3 function. A second series of truncated mutants were constructed with the N-terminal starting at S68, G94 and A103. All of these mutants were functional. In full length mUT-A3, deleting residues 103 to 113 (mUT-A3-Δ103-113) prevented urea uptake. When expressed in non-polarised MDCK cells, mUT-A3-Δ103-113 was trafficked to the plasma membrane and demonstrated

a distribution pattern similar to wild-type mUT-A3. Taken together these results suggest that the 8-aa region between residues 103 and 113 is required for normal transport function but is not linked to protein trafficking.
To investigate the role of the C-terminus, a series of truncation mutants were constructed. mUT-A3 has a predicted open reading frame of 460 amino acids. We inserted stop codons at residues 285, 315, 409, 429, 449 and 456. Urea uptake was not observed in oocytes expressing the E285X, I315X, W409X, Y429X V449X mutants. However, deleting the final 4 amino acids (K456X) did not reduce urea uptake compared to full length mUT-A3. These results suggests the 7aa between residues 450–456 are important for urea transport, although the precise role of this region in mUT-A3 function still needs to clarified.

Stewart GS *et al.* (2004). *Am J Physiol* 286, F979-F987.

Fenton RA *et al.* (2000). *Am J Physiol* 279, C1425-C1431.

The Financial support of Kidney Research UK is gratefully acknowledged.

Where applicable, the authors confirm that the experiments described here conform with the Physiological Society ethical requirements.

PC32

Lack of evidence *in vivo* for vagally mediated remote effects of *Escherichia coli* heat stable (STa) enterotoxin on jejunal fluid absorption

M.L. Lucas, N.W. Duncan, N.F. O'Reilly, T.J. McIlvenny and Y.B. Nelson

Division of Neuroscience & Biomedical Systems, Institute of Biological & Medical Science, University of Glasgow, Glasgow, UK

Heat stable (STa) enterotoxin from *E. coli* reduces absorption from the jejunum of the anaesthetised rat. STa is claimed (1) remotely to reduce fluid uptake since ileal perfusion with STa apparently reduces jejunal fluid absorption but not after cervical vagotomy. In view of likely cardiovascular effects of vagotomy on uptake and of reflexes caused by ileal perfusion, remote effects of STa were re-examined. Fluid uptake from jejunal loops was measured in anaesthetised (70 mg/kg i.p. Sagatal) unfasted Sprague Dawley rats (2). Twenty five cm loops were perfused with bicarbonate solution (150 mM). The vagus was intact, or sectioned at the neck or below the diaphragm. Completeness of sub-diaphragmatic section was determined by histology. Adequacy of function of isolated vagi were shown by effects of vagal stimulation on respiration and gastric secretion. Results are expressed as the mean and standard error, with the number of animals given. One loop was used per experiment. Significance was calculated after Dunnet's correction for multiple comparisons; $P < 0.01$.
Normal absorption experiments were intercalated with the vagotomy series, to confirm the activity of the STa. In these experiments, STA reduced fluid absorption in the jejunum from 81.6 ± 12.0 (8) µl/cm/h to 23.4 ± 4.2 (7) µl/cm/h. Control net jejunal fluid absorption of 79.5 ± 14.0 (7) µl/cm/h did not differ from absorption after cervical vagotomy of 75.6 ± 6.0 (6) µl/cm/h or after abdominal vagotomy of 76.1 ± 6.6 (8) µl/cm/h. The creation and perfusion of ileal loops without STa did nothing to net jejunal fluid absorption. *E. coli* STa added to ileal loops had no remote effect on jejunal fluid absorption as absorption was 94.4 ± 3.4 (7) µl/cm/h with saline and 89.3 ± 8.4 (6) µl/cm/h when STa (80 ng/ml) was included in the ileal loop. There was therefore no evidence for the remote effect of STa that has been claimed. The lack of a remote effect of STa on fluid movement confirms earlier observations (3) and supports the concept of a lack of vagally mediated fluid secretion being a factor in *E. coli* STa-mediated alterations in net fluid absorption.

Rolfe V & Levin RJ (1999). Gut 44, 615-619.

Lucas ML, Thom MMM, Bradley JM, O'Reilly NF, McIlvenny TJ & Nelson YB (2005). J Membr Biol 206, 29–42.

Hubel KA, Renquist KS & Varley G (1991). J Auton Nerv Syst 35, 53-62.

The authors are grateful to the Chancellor's Fund, the University of Glasgow for support.

Where applicable, the authors confirm that the experiments described here conform with the Physiological Society ethical requirements.

PC33

Vectorial transport by Capan-1 cells: a model for human pancreatic ductal bicarbonate secretion

A. Szucs[1], I. Demeter[1], G. Ovari[1], B. Burghardt[1], R.M. Case[2], M.C. Steward[2] and G. Varga[1]

[1]Molecular Oral Biology Research Group, Department of Oral Biology, Semmelweis University and Hungarian Academy of Sciences, Budapest, Hungary and [2]Faculty of Life Sciences, University of Manchester, Manchester, UK

Human pancreatic ducts secrete a bicarbonate-rich fluid but our knowledge of the secretory process is based mainly on animal models. Our aim was to determine whether the bicarbonate transport mechanisms in Capan-1, a human pancreatic ductal cell line are similar to those previously identified in guinea-pig pancreatic ducts.
The expression of potential key transporters and receptors was compared in normal human pancreas and cultured Capan-1 cells by RT-PCR. Monolayers of Capan-1 cells were grown on Transwell-COL PTFE membranes. To estimate transmembrane and transcellular bicarbonate movements, intracellular pH (pH_i) was monitored by microfluorometry using BCECF, a pH-sensitive fluoroprobe. Bicarbonate secretion was estimated from the initial rate of decrease in pH_i following inhibition of basolateral bicarbonate uptake by EIPA and H2DIDS.
By RT-PCR we found that pNBC1, NHE1, AE2, AE3, SLC26A6 transporters, CFTR channel and secretin, VPAC1, P2Y1,2,4,6 receptors were expressed both in normal human pancreas and in Capan-1 cells. Capan-1 cells grown on permeable supports formed confluent, polarized monolayers with well developed tight junctions. The recovery of pH_i from an acid load, induced by a short $NH4^+$ pulse, was mediated by Na^+-dependent transporters located exclusively at the basolateral membrane. One was independent of bicarbonate and blocked by EIPA (probably NHE1) while the other was bicarbonate-dependent and blocked by H2DIDS (probably pNBC1). Simultaneous administration

of basolateral EIPA and H2DIDS led to an immediate, pronounced decrease in pH_i (0.067 ± 0.003 pH/min; mean ± SEM; n=5) compared to untreated control. Bumetanide-sensitive recovery of pH_i during the NH_4^+ pulse was attributed to the presence of NKCC1. Changes in pH_i following blockade of basolateral bicarbonate accumulation confirmed that the cells achieve vectorial bicarbonate secretion. Dose-dependent increases in bicarbonate secretion were observed in response to stimulation of both secretin and VPAC receptors. The initial decrease in pH_i was accelerated by apical ATP (0.104 ± 0.004 pH/min; n=4) or UTP and inhibited by basolateral ATP (0.009 ± 0.001 pH/min; n=5) or UTP administration.

In conclusion, in Capan-1 cells NBC and NHE, localised exclusively at the basolateral membrane, are the key transporters involved in the maintenance of pH_i both during cellular acidification and during transcellular bicarbonate secretion. Extracellular purinergic activation induces differential effects, stimulation at the apical side, and inhibition on the basolateral side. Bicarbonate secretion in guinea-pig ducts and Capan-1 cell monolayers share many common features, suggesting that the latter is an excellent model for studies of human pancreatic bicarbonate secretion.

Supported by Wellcome Trust, the Royal Society, the Hungarian Scientific Research Fund (49058) and the Hungarian Medical Research Council (350/2003).

Where applicable, the authors confirm that the experiments described here conform with the Physiological Society ethical requirements.

PC34

The rabbit proton—peptide cotransporter, PepT1, interacts with the sodium—hydrogen exchanger NHE3 and its regulatory factor NHERF2 when expressed in *Xenopus* oocytes

C.A.R. Boyd, K. Panitsas and D. Meredith

Physiology, Anatomy & Genetics, University of Oxford, Oxford, UK

PepT1 mediates the intestinal absorption and renal re-absorption of di- and tri-peptides and a great number of therapeutically active compounds (Daniel & Kottra, 2004). Recently we have shown that PepT1 forms a multimer when expressed in *Xenopus* oocytes (Panitsas *et al.* 2006) using coinjection of an epitope-tagged wild-type protein (PepT1-FLAG) and a non-functional mutant W294F-FLAG. However, we could not exclude the possibility that other proteins may also be involved. To further investigate this, we have used rat intestinal RNA depleted of PepT1 message to see if there are other protein(s) expressed that could be involved.

PepT1-FLAG was expressed in *Xenopus* oocytes as previously described (Panitsas *et al.* 2006), either alone or by coinjection as described in the figure legend. Rat intestinal RNA was prehybridised with antisense oligonucleotides to rat PepT1, NHE3 and NHERF2 using the method described by Fei *et al.* (1994). Both membrane expression and the transport were determined by luminometry and uptake of 0.4μM [^{3}H]-D-Phe-L-Gln, respectively, using techniques previously described (Panitsas *et al.* 2006). Data are means ± SEM of n oocyte preparations.

Figure 1A shows the ability of co-injected PepT1-depleted intestinal RNA to reverse the inhibition of W294F-PepT1 on PepT1-FLAG, suggesting that there is a protein normally expressed in intestine that interacts with PepT1. Figure 1B shows that prehybridising the intestinal RNA with antisense oligonucleotides to the candidate proteins of the Na^+—H^+ exchange system, NHE3 and NHERF2, abolishes the reversal of the inhibition seen in Fig. 1A, suggesting that these proteins are involved.

Western blotting of immunopurified PepT1-FLAG (data not shown, n=3) gave bands which were consistent with a range of molecular complexes of PepT1 ranging from monomers to tetramers. In addition there were bands visible that were not multiples of the expected PepT1 monomer size of 76kDa (at 88, 156 and 262KDa), which could represent heteromultimers of PepT1 with other protein species. Further studies such as co-immunoprecipitation will be required to elucidate whether PepT1 and NHE3 and/or NHERF2 form a physical association or a functional one.

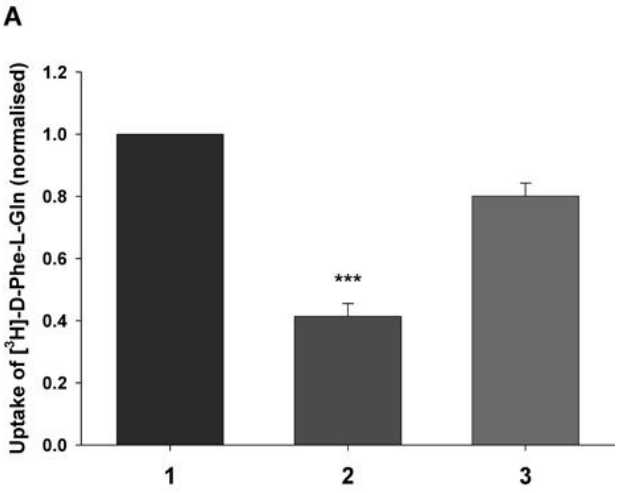

Figure 1A. Uptake of D-Phe-L-Gln normalised to transporter surface expression in *Xenopus* oocytes expressing (1) PepT1-FLAG, (2) PepT1-FLAG and W294F-PepT1, or (3) PepT1-FLAG and W294F-PepT1 when coinjected with PepT1-depleted intestinal RNA (*** $p<0.001$, Student's t test, n=13).

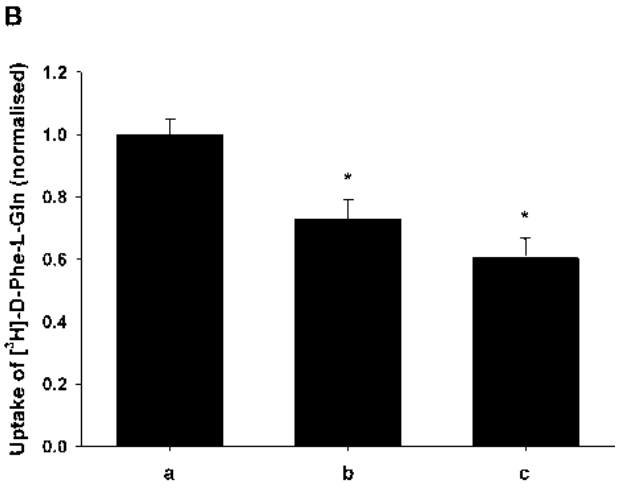

Figure 1B. Uptake of D-Phe-L-Gln normalised to transporter surface expression after coinjection of (a) PepT1-FLAG, W294F-PepT1 and PepT1-depleted intestinal RNA, additionally prehybridised with (b) NHE3 or (c) NHERF2 antisense oligonucleotides (* $p<0.05$, Student's t test, $n\geq3$).

Daniel H & Kottra G (2004). *Pflugers Arch* **447**, 610-618.

Panitsas K-E *et al.* (2006). *Pflugers Arch* (in press).

Fei YJ *et al.* (1994). *Nature* **368**, 563-566.

We thank the Wellcome Trust for their generous support.

Where applicable, the authors confirm that the experiments described here conform with the Physiological Society ethical requirements.

PC35

Structure–activity studies of fluorescein derivatives as potentiators of the CFTR Cl^- channel

Z. Cai[1], O. Moran[2], S.M. Husbands[3] and D.N. Sheppard[1]

[1]Department of Physiology, Bristol University, Bristol, UK, [2]Istituto di Biofisica, CNR, Genoa, Italy and [3]Department of Pharmacy and Pharmacology, University of Bath, Bath, UK

The fluorescein derivative phloxine B (2',4',5',7'-tetrabromo-4,5,6,7-tetrachlorofluorescein) is a potent modulator of the cystic fibrosis transmembrane conductance regulator (CFTR) Cl^- channel [1,2]. Nanomolar to low micromolar concentrations of phloxine B potentiate CFTR Cl^- currents, whereas higher concentrations ($\geq 10\,\mu M$) inhibit CFTR. To understand better channel potentiation by fluorescein derivatives, we studied bengal rose B (2',4',5',7'-tetrabromo-4,5,6,7-tetraiodofluorescein), ethyl eosin (2',4',5',7'-tetrabromoeosin ethyl ester), eosin Y (2',4',5',7'-tetrabromofluorescein), TCF (4,5,6,7-tetrachlorofluorescein), DCF (2',7'-dichlorofluorescein) and fluorescein using excised inside-out membrane patches from C127 cells expressing wild-type human CFTR. We also employed molecular docking to study the interaction of fluorescein derivatives with CFTR using a head-to-tail dimer model of CFTR's nucleotide-binding domains (NBDs) [3]. When added to the intracellular solution, with the exception of TCF and fluorescein that lack halogens in the xanthene moiety of the molecule, all other fluorescein derivatives potentiated CFTR Cl^- currents with the rank order of affinity: bengal rose B (K_d, 0.32 μM) > eosin Y (K_d, 0.62 μM) > ethyl eosin (K_d, 1.72 μM) > phloxine B (K_d, 2.78 μM) > DCF (K_d, 36.24 μM). Single-channel studies demonstrated that fluorescein derivatives augment CFTR Cl^- currents by increasing open probability (P_o, $P < 0.05$, n = 6–15) with phloxine B (1 μM) and eosin Y (1 μM) both prolonging mean burst duration (MBD, $P < 0.05$) without changing interburst interval (IBI, $P > 0.05$), and DCF (20 μM) decreasing IBI ($P < 0.05$) without changing MBD ($P > 0.05$, n = 4–15). Molecular docking studies suggest that fluorescein derivatives bind at the interface of the NBD dimer primarily by hydrophobic interactions. They also suggest that the putative binding sites involve sequences from both NBD1 and NBD2 and are distinct from the two ATP binding sites. Interestingly, evaluation of the binding free energy implies that fluorescein derivatives bind tighter to NBD1. We conclude that (i) halogens in the xanthene moiety of the molecule have essential roles for CFTR potentiation and different halogens have distinct effects on channel gating; (ii) chlorines in the benzene ring of the molecule enhance potency; (iii) the carboxylic group in the benzene ring plays little role in potentiation, but is a key determinant of CFTR inhibition; and (iv) fluorescein derivatives may potentiate CFTR Cl^- channel by stabilising the formation of the NBD dimer.

Bachmann A *et al.* (2000). *Br J Pharmacol* 131, 433-440.

Cai Z & Sheppard DN (2002). *J Biol Chem* 277, 19546-19553.

Moran O *et al.* (2005). *Cell Mol Life Sci* 62, 446-460.

Supported by the CF Trust and Italian Cystic Fibrosis Research Foundation (FFC).

Where applicable, the authors confirm that the experiments described here conform with the Physiological Society ethical requirements.

PC36

Basolateral ATP activates Cl^- secretion and Na^+ reabsorption in A6 epithelia

D.J. Jans[1], C. Balut[2], W. Van Driessche[1], P. Steels[1] and E. Van Kerkhove[1]

[1]Laboratory of Physiology, Hasselt University, Diepenbeek, Belgium and [2]Laboratory of Biophysics, International Centre of Biodynamics, Bucharest, Romania

The present study investigated the *in vitro* effects of extracellular ATP when applied to the basolateral border of renal epithelial cells in culture. We used the A6 epithelium cell line, derived from the distal renal tubules of the South-African clawed frog *Xenopus laevis*, as a model for the principal cells of the cortical collecting duct that exhibits both Na^+ reabsorption and Cl^- secretion in response to specific agonists. Epithelial polarisation was facilitated on permeable Anopore filter supports (pore size 0.2 μm). We continuously monitored the changes in transepithelial conductance (G_T) and short-circuit current (I_{sc}). Data are represented as means ± S.E.M. Upon the addition of ATP (5 μM) to the basolateral border, I_{sc} rapidly increased in a biphasic manner with an initial rapid increase from 1.1 ± 0.2 to 3.0 ± 0.4 $\mu A/cm^2$ with a parallel rise in G_T from 0.13 ± 0.01 to 0.15 ± 0.01 mS/cm^2 (N=6). Both increases were transient and partly recovered within 3 min. A second rise was observed for both parameters, albeit with a much slower time course, reaching a maximum ca. 20 min after the addition of ATP for G_T at 0.16 ± 0.02 mS/cm^2 and for I_{sc} at 5.5 ± 0.5 $\mu A/cm^2$. In the presence of amiloride (50 μM), the second phase of the increases in G_T and I_{sc} was completely abolished, whereas the initial rapid response remained. This indicates that the second phase of the changes in G_T and I_{sc} reflect Na^+ transport from the apical to the basolateral border. When substituting Cl^- for SO_4^{2-} in the basolateral bath, the first phase was overruled, whereas the second phase was still expressed. This is consistent with the process of Cl^- transport from the basolateral to the apical compartment during the first phase of the increases in G_T and I_{sc}. Our observations indicate that basolateral ATP elicits the immediate activation of Cl^- secretion followed by a much slower activation of Na^+ reabsorption. In a previous study (1), we observed similar responses in transepithelial transport during hypotonicity, suggesting that ATP, released across the basolateral border of the epithelium in response to cell swelling, underlies the biphasic increases of I_{sc} and G_T in these conditions (2). Further investigations are required to identify the receptors and the signal transduction pathways involved.

Jans D et al. (2000). *Pflügers Arch* 439, 504-512.

Jans D *et al.* (2002). *J Physiol* 545, 543-555.

This work was supported by the Fonds voor Wtenschappelijk Onderzoek Vlaanderen, Krediet aan Navorsers, Project FWO-V-1.5.215.05.

Where applicable, the authors confirm that the experiments described here conform with the Physiological Society ethical requirements.

PC37

Apical membrane targeting of ROMK2 (Kir1.1b) is independent of N-linked glycosylation

V.M. Collins[2,1], G.J. Cooper[2] and S.J. White[1]

[1]Institute of Membrane & Systems Biology, University of Leeds, Leeds, West Yorkshire, UK and [2]Department of Biomedical Science, University of Sheffield, Sheffield, South Yorkshire, UK

The Kir1.1 family of inwardly rectifying K^+ channels (ROMK 1-3: Kir1.1 a-c) mediate K^+ secretion across the apical membranes of the thick ascending limb and distal nephron (Hebert et al. 2005). However, the mechanisms that determine apical membrane targeting of Kir1.1 are not understood. N-Glycans determine surface expression of a number of membrane proteins (Muth & Caplan, 2003) and Kir1.1 contains a single glycosylation consensus sequence (NXS/T) at residues 98-100. In this study, we investigated the importance of glycosylation in membrane targeting of Kir1.1b.

Filter-grown monolayers of MDCK type I cells stably expressing EGFP-Kir1.1b (WT) were treated overnight with cycloheximide (CX: 20 μg/ml) and allowed to recover for 3, 6 or 24 h either in the absence or presence of 10 μg/ml tunicamycin (TM) to inhibit glycosylation (n = 3-5 separate experiments). In a second series of experiments, monolayers of MDCK type II cells were transfected with cDNA coding for WT or a mutant (N98Q: made by QuickChange® mutagenesis) lacking the glycosylation site (n = 3-5 separate transfections). Intracellular localisation of EGFP-fusion proteins was determined by fluorescence confocal microscopy in conjunction with labelling of the apical membrane with TRITC conjugated wheat germ agglutinin (WGA) or peanut agglutinin (PNA) for MDCK I or II, respectively.

In monolayers treated with CX for 17 h, WT levels were greatly reduced and fluorescence was not evident at the apical pole of the cells. When cells were washed and incubated in CX-free media for a further 3, 6 or 24 h, the levels of fluorescence progressively recovered to control levels, and co-localised with WGA, confirming targeting of the fusion protein to the apical membrane. Following incubation with TM, the levels of WT fluorescence at 3, 6 and 24 h were similar to that of untreated controls, but, with time, the predominant species of the protein shifted from the glycosylated (~70 kDa) form to the non-glycosylated (~67 kDa) form, confirmed by SDS-PAGE and Western blotting (Ortega *et al.* 2002). Nevertheless, the fusion protein was still expressed at the apical membrane. Transient expression of MDCK II cells with either WT or N98Q, resulted in fluorescence predominantly at the apical pole of the cells, colocalising with PNA.

We conclude that polarized membrane targeting of Kir1.1b is unaffected by either prevention of the addition of complex oligosaccharides by tunicamycin, or by elimination of the N-linked glycosylation motif, when expressed in either form of MDCK cell type. These findings indicate that Kir1.1b protein is transported to the apical membrane via a mechanism(s) independent of glycosylation of the channel *per se.*

Hebert SC *et al.* (2005). *Physiol Rev* **85**, 319-371.

Muth TR & Caplan MJ (2003). *Ann Rev Cell Dev Biol* **19**, 333-366.

Ortega B *et al.* (2002). *J Physiol* **528**, 5-13.

We thank Kidney Research UK for financial support and the White-Rose consortium for a postgraduate scholarship (VMC).

Where applicable, the authors confirm that the experiments described here conform with the Physiological Society ethical requirements.

PC38

Acute metabolic stress increases the K^+ conductance of human colonic crypts via activation of basolateral Ca^{2+}-sensitive, intermediate conductance K^+ channels (IK_{Ca})

A. Loganathan[2,3], J.E. Linley[2], P. Lodge[3], G. Sandle[2] and M. Hunter[1]

[1]Institute of Membrane and Systems Biology, University of Leeds, Leeds, UK, [2]Institute of Molecular Medicine, St James's University Hospital, Leeds, UK and [3]Department of Hepatobiliary Surgery, St James's University Hospital, Leeds, UK

Gut hypoxia during major surgery is associated with increased intestinal permeability, bacterial translocation, systemic sepsis and multi-organ failure. K^+ channel activation represents a common response to metabolic inhibition in a number of different cell types. Acute metabolic stress produced by 2,4dinitrophenol (DNP) and deoxyglucose (DG) activates large conductance K^+ channels in cardiovascular tissues, and small conductance K^+ channels in liver and biliary cell lines. In the T_{84} colonic adenocarcinoma cell line, mastoparan caused a 4-fold increase in paracellular permeability that was linked to increased basolateral membrane K^+ conductance. Thus, modulation of K^+ channel activity represents a potential target for reducing the risk of systemic sepsis due to hypoxic intestinal injury.

The aim of the current study was to determine whether acute metabolic stress leads to activation of basolateral K^+ channels in human colonic crypts.

Biopsies of normal sigmoid colonic mucosa were obtained from patients undergoing routine colonoscopy. Crypts were isolated by Ca^{2+} chelation (Bowley *et al.* 2003). Whole-cell K^+ currents were measured using the perforated patch-clamp technique (0.24mg/ml amphotericin in pipette), and single channel activity in the basolateral membrane was studied in the cell-attached configuration. Cells were exposed to 100μM DNP + 5mM DG to produce metabolic inhibition. Data are presented as mean ± 1 SEM, with n, the number of experiments, and were compared by Student's paired t test.

Metabolic inhibition stimulated whole-cell currents within 5 minutes, with an increase in whole-cell conductance from 1.45 ± 0.13nS to 3.29 ± 0.19nS ($P<0.005$; n = 11), and hyperpolarization of the cell membrane voltage from -67 ± 3mV to -80 ± 3mV ($P<0.025$), consistent with K^+ channel activation; these

effects were completely inhibited by the specific IK_{Ca} inhibitor, TRAM-34. In single channel recordings, metabolic inhibition increased IK_{Ca} activity; NPo, where N = number of channels and Po = open probability, increased from 0.58 ± 0.2 to 0.81± 0.3 ($p<0.05$, n=10)

In conclusion, metabolic stress activates basolateral K^+ channels (IK_{Ca}) in human colonic crypts, resulting in hyperpolarization of the membrane potential. Further studies are required to establish if IK_{Ca} stimulation is associated with an increase in paracellular permeabilility. If so established, specific K^+ channel blocking drugs may be of theraputic use in the prevention of systemic sepsis associated with gut hypoxia.

Bowley KA et al. (2003). *Gut* **52**,854-860.

Where applicable, the authors confirm that the experiments described here conform with the Physiological Society ethical requirements.

PC39

Use of giant liposomes to study the CFTR Cl^- channel

L.K. Hughes and D.N. Sheppard

Physiology, University of Bristol, Bristol, UK

The genetic disease cystic fibrosis (CF) is characterised by loss of transepithelial salt and water transport caused by malfunction of the cystic fibrosis transmembrane conductance regulator (CFTR) Cl^- channel. A novel strategy to restore transepithelial Cl^- transport to CF epithelia is to use artificial Cl^- transporters to transfer Cl^- across the apical membrane of these epithelia. During studies of one family of artificial transporters, we sought a method to investigate their transport properties in a cell-free system. Besides planar lipid bilayers, giant liposomes have been employed for single-channel studies of ion channels (Keller et al. 1988).

To evaluate the use of giant liposomes for electrophysiological studies, we studied wild-type human CFTR assessing the characteristics of the channel in this artificial environment. Using a modification of the method of Riquelme et al. (1990), we synthesised giant liposomes from the phospholipid asolectin by the dehydration/rehydration technique. For a source of wild-type human CFTR, we used membranes from Fischer rat thyroid (FRT) cells expressing wild-type human CFTR and incorporated them into liposomes by high-speed centrifugation. To study the behaviour of CFTR incorporated into giant liposomes, we used the excised inside-out configuration of the patch–clamp technique. We found that membrane patches excised from giant liposomes form high resistance seals (> 10 GΩ) that are stable over time and large voltage ranges and have baseline noise equal to or lower than that achieved with excised membrane patches from cell membranes.

Like CFTR Cl^- channels recorded in cellular membranes, CFTR reconstituted in giant liposomes formed Cl^- selective channels that were regulated by cyclic AMP-dependent phosphorylation and intracellular ATP. Upon excision of membrane patches from some giant liposomes, we observed large conductance Cl^- channels. However, no channel activity resembling CFTR was observed before the addition of ATP (1 mM) and PKA (75 nM; n = 4). In one membrane patch containing a single CFTR Cl^- channel, at –50 mV we measured a single-channel current amplitude of –0.46 pA at 27°C and –0.52 pA at 37°C using a Cl^- concentration gradient ($[Cl^-]_{intra}$ = 148 mM, $[Cl^-]_{extra}$ = 10 mM). At 37°C, the gating behaviour of this channel resembled that of CFTR in a cellular environment with bursts of openings interrupted by brief closures and separated by longer closures between bursts.

We interpret our data to suggest that CFTR incorporated into giant liposomes retains many of its characteristics. However, the different lipid environment influences channel behaviour. We will now use this technique to study the activity of other Cl^- transporters in a cell-free system.

Riquelme G et al. (1990). Biochemistry 29, 11215-11222.

Keller BU et al. (1988). Pflügers Arch 411, 94-100.

We thank Drs G. Riquelme (University of Chile) and O. Moran (Istituto di Biofisica, Genoa) for their valuable advice. Supported by the BBSRC and CF Trust.

Where applicable, the authors confirm that the experiments described here conform with the Physiological Society ethical requirements.

PC40

Nitric oxide reduces the promoter activity of *SLC29A1* gene for equilibrative nucleoside transporter 1 (hENT1) in human fetal endothelium from gestational diabetes

M. Farias[1], R. San Martin[1], C. Puebla[1], J.D. Pearson[2], M. Pastor-Anglada[3], P. Casanello[1] and L. Sobrevia[1]

[1]Cellular and Molecular Physiology Laboratory (CMPL), Department of Obstetrics & Gynaecology, Medical Research Centre (CIM), School of Medicine, Pontificia Universidad Catolica de Chile, Santiago, Chile, [2]Biomedical Sciences Division, Kings College London, University of London, London, UK and [3]Department of Biochemistry and Molecular Biology, Faculty of Biology, Universitat de Barcelona, Barcelona, Spain

Adenosine is a vasodilator in most vascular beds, an effect depending on its extracellular concentration which is efficiently regulated by nucleoside membrane transporters. Uptake of this nucleoside in human umbilical vein endothelial cells (HUVEC) is achieved by the human equilibrative, Na^+-independent nucleoside transporters 1 (hENT1) and hENT2 (San Martín & Sobrevia, 2006). hENT1 expression and transport activity are reduced in HUVEC isolated from pregnancies with gestational diabetes, an effect associated with increased L-arginine uptake and nitric oxide (NO) synthesis (Vásquez et al. 2004). However, regulatory mechanisms at transcriptional or post-transcriptional level accounting for this effect of gestational diabetes have not been reported. We studied the involvement of NO in the regulation of hENT1 expression and activity in HUVEC.

Adenosine transport ([^{3}H]adenosine, 2 μCi/ml, 5 s, 22°C) was measured in passage 2 cells in medium 199 (3.2 mM L-glutamine) in the absence or presence of nitrobenzylthioinosine (NBMPR, 0.1-10 μM), hypoxanthine (2 mM), N^G-nitro-L-arginine methyl ester (L-NAME, 100 μM), *S*-nitroso-N-acetyl-L,D-penicillamine (SNAP, 10 μM, NO donor) or in cells infected with an adenovirus containing a siRNA sequence targeting eNOS (Ad-eNOS). hENT1 mRNA was determined by RT-PCR, and protein

abundance by Western blot. Four fragments of upstream region of *SLC29A1* gene (for hENT1) up to -3198, -2154, -1114 and -795 bp from ATG were cloned into pGL3-Basic and transfected by electroporation (320 V, 30 ms).
The maximal velocity (V_{max}) of hENT1-mediated adenosine transport was reduced in HUVEC from gestational diabetes compared with normal cells (0.69 ± 0.1 vs 1.37 ± 0.1pmol/μg protein/s, respectively; P=0.0003, unpaired Student's t test, mean ± S.E.M., n=7). This effect of gestational diabetes was blocked (P=0.001) by L-NAME (V_{max} = 2.19 ± 0.22 pmol/μg protein/s). SNAP reduced adenosine transport in normal cells (0.49 ± 0.06 pmol/μg protein/s), but not in diabetic cells (0.50 ± 0.05 pmol/μg protein/s). A reduction (60 ± 5%) of hENT1 protein abundance was found in diabetic cells, an effect blocked by L-NAME and mimicked by SNAP (67 ± 10%) in normal cells. Infection with Ad-eNOS increased hENT1 mRNA level (1.8- and 3-fold), protein abundance (2- and 4-fold) and adenosine uptake (1.8- and 2.8-fold) in normal and diabetic cells, respectively, compared with respective controls. Transcriptional activity of *SLC29A1* promoter was increased (1.4-fold) by transfection of pGL3-hENT1^{-1114}, but was reduced (48 ± 4%) by pGL3-hENT1^{-2154} in HUVEC from gestational diabetes. Reduced promoter activity by pGL3-hENT1^{-2154} was blocked by L-NAME. Thus, reduced adenosine transport in gestational diabetes may result from a lower transcriptional *SLC29A1* promoter activity through a NO-dependent mechanism.

San Martín R & Sobrevia L (2006). *Placenta* **27**, 1-10.

Vasquez G et al. (2004). *J Physiol* **560**, 111-122.

Supported by FONDECYT 1030781, 1030607, 7050030 (Chile), SAF2005-01259 (Spain). M. Farías holds CONICYT- and Faculty of Medicine-PhD fellowships (Chile).

Where applicable, the authors confirm that the experiments described here conform with the Physiological Society ethical requirements.

PC41

CFTR regulation by intracellular pH: kinetic modelling of channel gating

J. Chen, Z. Cai and D.N. Sheppard

Physiology, University of Bristol, Bristol, UK

The cystic fibrosis transmembrane conductance regulator (CFTR) is a Cl^- channel with complex regulation. In previous work, we demonstrated that intracellular pH (pH_i) modulates CFTR activity by altering channel gating (Chen et al. 2003). To understand the underlying mechanism, we studied CFTR channel gating at pH_i values from 5.8 to 8.8 using excised inside-out membrane patches from C127 cells expressing recombinant wild-type human CFTR that each contain only a single CFTR Cl^- channel. The pipette (external) solution contained 10 mM Cl^- at pH 7.3, and the bath (internal) solution contained 147 mM Cl^-, PKA (75 nM) and ATP (0.3 mM); voltage was –50 mV.
Analyses of dwell time histograms demonstrated that channel gating was best described by one open state and two closed states at all pH_i values tested. Burst analyses demonstrated that pH_i decreased mean burst duration (MBD) as pH_i increased (e.g. pH_i 5.8, MBD = 357 ± 32 ms; pH_i 7.3, MBD = 133 ± 4 ms; pH_i 8.8, MBD = 93 ± 6 ms; n ≥ 4; $p < 0.05$). In contrast, pH_i had complex effects on interburst interval (e.g. pH_i 5.8, IBI = 515 ± 56 ms; pH_i 7.3, IBI = 155 ± 5 ms; pH_i 8.8, IBI = 144 ± 10 ms; n ≥ 4). To understand better how pH_i changes CFTR channel gating, we used QuB software and the $C_1 \leftrightarrow C_2 \leftrightarrow O$ and $C_1 \leftrightarrow O \leftrightarrow C_2$ kinetic schemes (C_1, long closed state; C_2, brief closed state; O, open state) to model channel gating. In the $C_1 \leftrightarrow C_2 \leftrightarrow O$ gating scheme, pH_i predominantly modulated transitions between the C_1 and C_2 states. In the $C_1 \leftrightarrow O \leftrightarrow C_2$ kinetic scheme, pH_i markedly altered transitions between the C_1 and O states, while acidic pH_i also altered transitions between the O and C_2 states. These data suggest that pH_i regulates MBD and IBI primarily by altering transitions between the first two states in both kinetic schemes.
Because ATP binding and hydrolysis at two ATP binding sites controls channel gating, we assume that ATP molecules drive transitions between the different gating states C_1, C_2 and O. Thus, we derived the relationship between open probability (P_o) and [MgATP] using the $C_1 \leftrightarrow C_2 \leftrightarrow O$ and $C_1 \leftrightarrow O \leftrightarrow C_2$ kinetic schemes. By examining whether the relationship between P_o and [MgATP] is well fitted by the Michaelis-Menten equation, our data demonstrate that if only one ATP molecule controls channel gating, C_1 is the site of interaction with ATP in both the kinetic schemes. However, if two ATP molecules control channel gating, only the $C_1 \leftrightarrow O \leftrightarrow C_2$ kinetic scheme describes the interaction of CFTR with ATP and ATP interacts with both closed states C_1 and C_2 in this kinetic scheme. Based on these data, we proposed a kinetic model with two ATP molecules interacting with CFTR to explain how pH_i modulates CFTR gating.

Chen J-H et al. (2003). J Gen Physiol 122, 23a.

Supported by the CF Trust and the University of Bristol.

Where applicable, the authors confirm that the experiments described here conform with the Physiological Society ethical requirements.

PC42

Regulation of the epithelial sodium channel by phosphatidylinositol 4,5-bisphosphate

C.R. Campbell, D.I. Cook and A. Dinudom

School of Medical Sciences, University of Sydney, Sydney, NSW, Australia

Epithelial Na^+ channels (ENaC) control sodium and fluid homeostasis and regulate blood pressure. In addition to being tightly regulated by well-known hormonal and homocellular factors, recent studies in A6 epithelial cells indicate that ENaC activity may be influenced by a membrane lipid [1,2], phosphatidylinositol 4,5-bisphosphate (PIP2). The detail mechanism by which PIP2 regulates ENaC activity is still not known.
In this study we used whole cell patch-clamp techniques to investigate the physiological role of PIP2 in regulating transepithelial Na^+ absorption. Amiloride-sensitive Na^+ conductance was measured in duct cells prepared from mandibular glands of Quackenbush mice post mortem [3]. After holding the whole-cell configuration for 3 min, the whole-cell current was measured. The observed difference between the currents with and

without 100 μM amiloride was used to calculate the amiloride-sensitive Na^+ conductance.
Under control conditions, the amiloride-sensitive chord conductance of the duct cells was 306.4 ± 33.4 pS (n = 19). Addition of an antibody directed against PIP2 (60 nM) to the pipette solution reduced the amiloride-sensitive conductance by 44.5% to 170.1 ± 12.5 pS (n = 8, P < 0.05) whereas heat-inactivated PIP2 antibody was without effect. Therefore, PIP2 activity may contribute to maintenance of ENaC function in duct cells. The effect of PIP2 on ENaC is believed to be mediated via ENaC β and γ N-termini [4]. Inclusion in the pipette solution of either β- or γ-ENaC N-terminal peptides containing the consensus PIP2 binding sites inhibited ENaC activity by more than 60%. Interestingly, inclusion of 25 μM PIP2 in the pipette solution prevented ENaC from being downregulated by high cytosolic Na^+ concentration. The mechanism by which PIP2 inhibits Na^+ feedback regulation of ENaC in the duct cell is currently under investigation.

Ma HP, Saxena S & Warnock DG (2002). J Biol Chem 277, 7641-7644.

Yue G, Malik B, Yue G & Eaton DC (2002). J Biol Chem 277, 11965-11969.

Dinudom A, Harvey KF, Komwatana P, Young JA, Kumar S & Cook DI (1998). Proc Natl Acad Sci U S A 95, 7169-7173.

Kunzelmann K, Bachhuber T, Regeer R, Markovich D, Sun J & Schreiber R (2005). FASEB J 19, 142-143.

This project is supported by a the National Health and Medical Research Council of Australia.

Where applicable, the authors confirm that the experiments described here conform with the Physiological Society ethical requirements.

PC43

Defective flow-induced Ca^{2+} signalling and ciliary protein localization in primary ADPKD cyst epithelial cells with a novel in-frame codon deletion in the PKD1 gene

S.L. Alper[1], R. Bacallao[3], A. Wandinger-Ness[4], S. Rossetti[2], P.C. Harris[2] and C. Xu[1]

[1]Medicine, Beth Israel Deaconess Medical Center, Harvard Medical School, Boston, MA, USA, [2]Medicine and Biochemistry, Mayo Medical School, Rochester, MN, USA, [3]Medicine, Indiana Univ Medical School, Indianapolis, IN, USA and [4]Anatomy and Cell Biology, Univ New Mexico School of Medicine, Albuquerque, NM, USA

The autosomal dominant polycystic kidney disease (ADPKD) genes polycystin-1 (PC1) and polycystin-2 (PC2) colocalize with other polycystic kidney disease genes in the apical monocilium of mouse and dog renal epithelial cells. PC1-deficient, precystic, embryonic mouse collecting duct cells in primary culture show impaired PC2-dependent ciliary mechanosensation. However, most human ADPKD kidneys express normal or elevated levels of apparently full-length PC1 and PC2 polypeptides. We have localized PC1 and PC2 in the monocilium of normal human renal (NK) epithelial cells in confluent primary culture. However, cilia of ADPKD cyst cells from a patient with the novel PC1 mutation ΔL2433 were devoid of detectable PC1, and 70% of cilia lacked PC2, despite normal total cell levels of both polypeptides. 34% of confluent NK cell coverslips exposed to 'physiological' laminar shear stress of 0.75 or 2.3 dyn cm^{-2}, respectively, increased $[Ca^{2+}]_i$ by 56+10 nM (n=22) or 48+9 nM (n=13) above resting levels (149+6 nM, n=61; P<0.01 for both). 80% of confluent NK coverslips exposed to 'diuretic' or supraphysiologic shear stresses of 10 or 35 dyn cm^{-2}, respectively, increased $[Ca^{2+}]_i$ by 207+65 nM (n=13) or 252+43 nM (n=15, P< 0.0001 for both). This flow-induced, transient $[Ca^{2+}]_i$ increase required both extracellular Ca^{2+} and release from intracellular Ca^{2+} stores, and was inhibited by 3 μM GsMTx-IV, 30 μM ryanodine and 20 μM 2-APB, but not by phospholipase C inhibitor U73122 (10 μM). ADPKD cyst cells, in contrast, lacked flow-sensitive $[Ca^{2+}]_i$ signalling and exhibited reduced ER Ca^{2+} stores and store-depletion-operated Ca^{2+} entry, but retained near-normal Ca^{2+}_i responses to angiotensin II and to vasopressin. Expression of wildtype and mutant CD16.7-PKD1(115-226) fusion proteins revealed within the C-terminal 112 aa of PC1 a ciliary targeting signal active in NK and cyst cells, and independent of the coiled-coil domain. However, the coiled-coil domain was required for CD16.7-PKD1(115-226) expression to accelerate decay of the flow-induced Ca^{2+} signal in NK cells. These data provide evidence for ciliary dysfunction in human ADPKD, and support a role for that dysfunction in disease pathogenesis.

Supported by NIH F32-DK69049 and NIH R01-DK57662 grants.

Where applicable, the authors confirm that the experiments described here conform with the Physiological Society ethical requirements.